



Fibroblast growth factor 7 alleviates myocardial infarction by improving oxidative stress via PI3K α /AKT-mediated regulation of Nrf2 and HXK2

Lin Mei^{a,b,c,1}, Yunjie Chen^{d,1}, Peng Chen^{a,1}, Huinan Chen^c, Shengqu He^c, Cheng Jin^c, Yang Wang^e, Zhicheng Hu^c, Wanqian Li^f, Litai Jin^c, Weitao Cong^{c,**}, Xu Wang^{c,*}, Xueqiang Guan^{a,***}

^a Department of Cardiology, The Second Affiliated Hospital and Yuying Children's Hospital of Wenzhou Medical University, Wenzhou, 325000, PR China

^b Department of Pharmacy, Xiamen Medical College, Xiamen, 361023, China

^c School of Pharmaceutical Science, Wenzhou Medical University, Wenzhou, 325000, PR China

^d Department of Pharmacy, Ningbo First Hospital, Ningbo, 315010, PR China

^e Department of Histology and Embryology, Institute of Neuroscience, Wenzhou Medical University, Wenzhou, 325000, China

^f Department of Pharmacy, Taizhou Municipal Hospital, Taizhou, 318000, PR China

ARTICLE INFO

Keywords:

FGF7
Myocardial infarction
Oxidative stress
Apoptosis
Nrf2
HXK2

ABSTRACT

Acute myocardial infarction (MI) triggers oxidative stress, which worsen cardiac function, eventually leads to remodeling and heart failure. Unfortunately, effective therapeutic approaches are lacking. Fibroblast growth factor 7 (FGF7) is proved with respect to its proliferative effects and high expression level during embryonic heart development. However, the regulatory role of FGF7 in cardiovascular disease, especially MI, remains unclear. FGF7 expression was significantly decreased in a mouse model at 7 days after MI. Further experiments suggested that FGF7 alleviated MI-induced cell apoptosis and improved cardiac function. Mechanistic studies revealed that FGF7 attenuated MI by inhibiting oxidative stress. Overexpression of FGF7 activates nuclear factor erythroid 2-related factor 2 (Nrf2) and scavenging of reactive oxygen species (ROS), and thereby improved oxidative stress, mainly controlled by the phosphatidylinositol-3-kinase α (PI3K α)/AKT signaling pathway. The effects of FGF7 were partly abrogated in Nrf2 deficiency mice. In addition, overexpression of FGF7 promoted hexokinase2 (HXK2) and mitochondrial membrane translocation and suppressed mitochondrial superoxide production to decrease oxidative stress. The role of HXK2 in FGF7-mediated improvement of mitochondrial superoxide production and protection against MI was verified using a HXK2 inhibitor (3-BrPA) and a HXKII VDAC binding domain (HXK2VBD) peptide, which competitively inhibits localization of HXK2 on mitochondria. Furthermore, inhibition of PI3K α /AKT signaling abolished regulation of Nrf2 and HXK2 by FGF7 upon MI. Together, these results indicate that the cardio protection of FGF7 under MI injury is mostly attributable to its role in maintaining redox homeostasis via Nrf2 and HXK2, which is mediated by PI3K α /AKT signaling.

1. Introduction

With the acceleration of population aging and the influence of unhealthy lifestyles, the prevalence of cardiovascular disease risk factors is increasing [1,2]. Myocardial infarction (MI) exhibits high morbidity and mortality [3]. Therefore, effective therapies must be urgently developed to prevent or treat MI and thereby improve the outcomes of patients.

Although therapies of reperfusion reduce the mortality, they don't prevent cardiomyocyte death caused by ischemia [4,5]. Massive cardiomyocyte death is the primary cause of MI-induced cardiac injury and heart dysfunction. Oxidative stress, which is elicited by acute myocardial ischemia, is an important trigger of cell death and affects pathophysiological processes of infarction [6]. During myocardial injury, production of oxidants is enhanced, and elimination of oxidants is

* Corresponding author.

** Corresponding author.

*** Corresponding author.

E-mail addresses: cwt97126@126.com (W. Cong), wang_xu2003@163.com (X. Wang), wzsgxq@163.com (X. Guan).

¹ Co-first authors.

decreased, which leads to an imbalance of the redox state. A persistent imbalance cause massive cardiomyocyte death, aggravates myocardial injury, and exacerbate cardiac dysfunction [7]. Therefore, maintenance of redox homeostasis by activating antioxidant factors and reducing oxidant production is considered a potential strategy for myocardial protection. However, few regulators with such dual functions.

Fibroblast growth factor 7 (FGF7) a member of the fibroblast growth factor family and has diverse biological functions, such as regulating cell differentiation, promoting mitosis, and inhibiting apoptosis [8–11]. During embryonic development, FGF7 is mainly distributed in the forebrain, interstitial tissue, and heart, and is especially highly expressed in ventricles and atria [12,13]. By contrast, FGF7 is down-regulated in human pathological cardiac tissues compared with normal tissues [14]. It is also a protective factor that reduces postoperative pericardial adhesions by promoting mesothelial regeneration, and was developed into a drug (Palifermin) to treat mucositis caused by chemotherapy/radiotherapy [15,16]. Moreover, it has been reported that FGF7 attenuates oxidative stress injury in tissue repair [9,10]. And FGF7 reportedly increases nuclear factor erythroid 2-related factor 2 (Nrf2) to protect against oxidative stress [11]. These indicate that FGF7 may elicit beneficial effects in the heart by regulating oxidative stress.

Nrf2, a redox-related transcription factor, is proposed to be an important target for regulating the expression and function of endogenous antioxidants such as Catalase, superoxide dismutases (SODs), and heme oxygenase (HO)-1 [17]. Nrf2 ameliorates cardiac injury by up-regulating protective antioxidant response element genes [18,19]. Although numerous inducers of Nrf2 have been discovered or developed as possible treatments to scavenge free radicals, they have limited effects on formation of free radicals.

Mitochondria is a main source of reactive oxygen species (ROS) [20]. Maintenance of mitochondrial homeostasis and reduction of ROS production is considered a potential strategy to mitigate oxidative stress-induced damage. Hexokinase II (HXK2) is a rate-limiting enzyme in glycolysis [21,22]. Growing evidence indicates that HXK2 plays a key role in maintaining mitochondrial function, which in turn ameliorates ROS production and cell death, via binding to mitochondria [23,24].

FGF7 regulates the phosphatidylinositol-3-kinase α (PI3K α)/AKT pathway [25,26], which is closely related to cell growth, migration, differentiation, proliferation, and metabolism in many diseases [27]. Increasing literature reports that activation of AKT protects against MI-induced injury [28–30], and AKT signaling promotes the nuclear accumulation of Nrf2 and thereby has an antioxidative function via ROS scavenging [31]. In addition, AKT phosphorylates HXK2 to increase its mitochondrial association, and thereby protects cardiomyocytes against ROS overproduction and apoptosis [23].

The present study aimed to determine whether FGF7 affects MI-induced cardiac injury and dysfunction, and to investigate whether the redox balance is involved in the mechanisms underlying the effects of FGF7.

2. Materials and methods

Please see the Major Resources Table in the Supplementary Data.

Detailed experimental methods are provided in the Supplementary Data.

2.1. Animal procedures

C57BL/6 mice and Nrf2 knockout mice (Nrf2-KO, C57BL/6 background [32]) aged 6 weeks were used in this study. The apex of the mouse heart was injected with 1×10^{11} vector genomes of a recombinant adeno associated virus (rAAV) serotype 9 carrying either FGF7 (rAAV-FGF7) or rAAV serotype 9 carrying either control vector (rAAV-LacZ) with the c-TNT promoter. Briefly, the left third, fourth and intercostal muscles were incised, and the left pleural cavity was opened to expose the heart after the mice were anesthetized. 10 μ L of rAAV

vector (5×10^{10} vector genomes per point) was injected near the apex of heart and the anterior left ventricle using a syringe (with a 29-G needle), respectively. Two weeks after the treatment, mice were used for further analysis. Nrf2-KO mice with rAAV treatment were applied by above procedure. rAAV-FGF7 and rAAV-LacZ were obtained from OBiO Technology (Shanghai) Corp., Ltd.

For inhibiting of AKT, mice were injected intraperitoneally with a PI3K inhibitor (LY294002, 2.5 mg/kg, Selleck) or saline from ligating the left anterior descending coronary artery (LAD) operation to 7 days after LAD operation.

2.2. Mice MI model establishment

Mice were performed by LAD to construct MI model. Briefly, mice were anesthetized and chest was opened to expose the hearts. Then, ligation of the LAD model was constructed by an 7-0 nylon suture. The sham group underwent the same operation but without ligation. Echocardiography was used to evaluate the mice cardiac function after 7 days, and experimental samples were harvested after euthanasia.

2.3. Echocardiography

Echocardiograms were acquired by a Vevo 1100 Ultrasound System (VisualSonics, Toronto, Canada). Echocardiography was performed after 1 week following LAD. The mice were anesthetized by using 1.5% isoflurane mixed in 1 L/min O₂. The heart rates were maintained at 400–500 beats per minute by adjusting the flow of isoflurane. Body temperature was maintained at 37.0 °C by a rectal temperature probe and heating blanket. The long-axis (M-mode) was used for analysis of systolic or diastolic ventricular diameter. Left ventricular fractional shortening (LVFS = [LVEDD - LVESD] \times 100/LVEDD) and left ventricular ejection fraction (LVEF = [LVEDV - LVESV] \times 100/LVEDV) were evaluated for analysis of systolic function. The Vevo LAB software (version 3.1.1) (VisualSonics, Toronto, Canada) was used for the subsequent analysis.

2.4. Isolation and culture adult mouse cardiomyocytes (ACMs) and adult mouse fibroblasts (ACFs)

ACMs and ACFs were from 8 to 12 weeks old C57BL/6 mice or MI mice were isolated as previously reported [33]. Isolated cardiomyocytes and fibroblasts were used for western bolt assays.

2.5. Isolation, culture and oxygen glucose deprivation (OGD) treatment of neonatal rat cardiomyocytes (NRCMs)

NRCMs were isolated from 1- to 2-day-old Sprague-Dawley (SD) rats according to previously method [34]. Briefly, the SD rat pups were rinsed rapidly in 75% ethanol solution for sterilization. Hearts were extracted and steeped ins cold DPBS (Gibco, 14190144). Tissues were minced with scissors (approximately 0.5–1 mm³), which were then placed into a tube containing trypsin medium [0.08% trypsin (Solarbio, T8150), 0.03% KCl (Sigma-Aldrich, V900068), 0.8% NaCl (Sigma-Aldrich, V900058), 0.1% D-(+)-Glucose (Sigma-Aldrich, G7021), 0.035% NaHCO₃ (Sigma-Aldrich, V900182) and 0.2% Hepes (Sigma-Aldrich, H3375)] with magnetic stirring (100 rpm for 8 min) in a 37 °C water bath.

After digestion, the suspension was placed on top of a gradient solution (Sigma, P4937). It was then centrifuged for 30 min at 3000 rpm. The cardiomyocytes were harvested from the newly layer. Finally, cardiomyocytes were plated in collagen (Sigma-Aldrich, C919) coated six well culture plates (5×10^5 cells per well), which consisted of DMEM/F-12 (Gibco, 11330032) supplemented with 1% penicillin/streptomycin and 10% FBS.

NRCMs were subjected to hypoxia (94% N₂, 1% O₂ and 5% CO₂) in an oxygen control cabinet (ESCO, Singapore). The model of OGD was

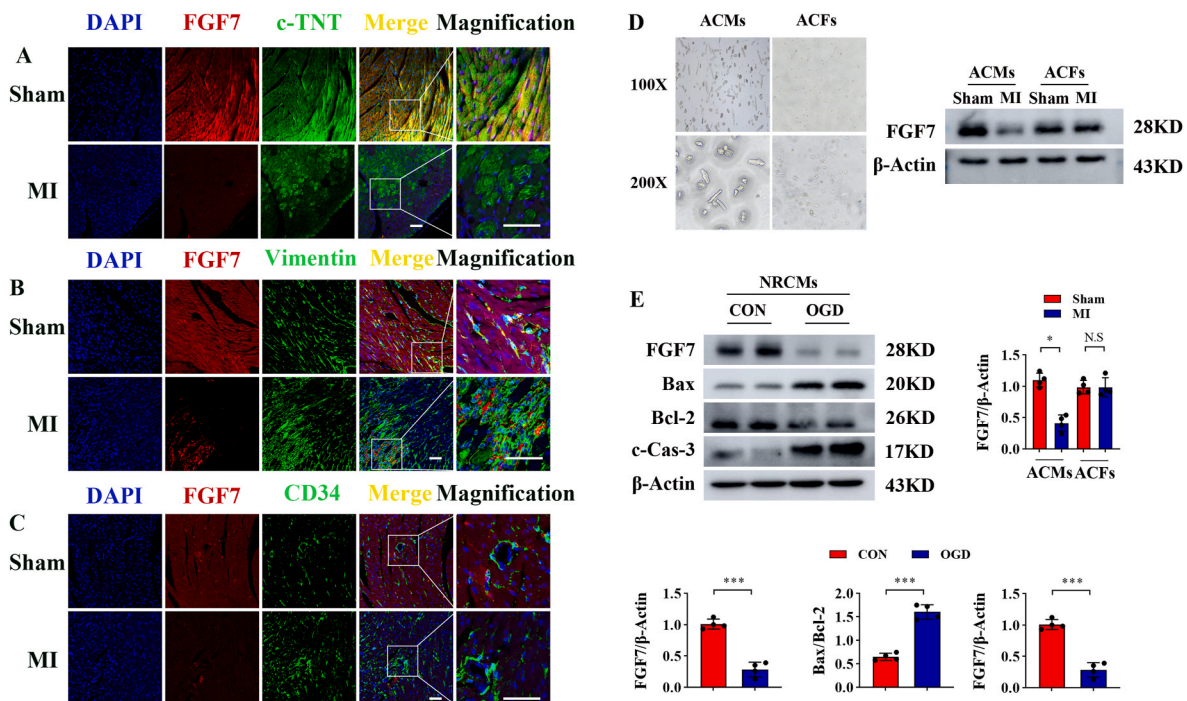


Fig. 1. FGF7 is downregulated in cardiomyocytes upon MI and oxygen-glucose deprivation (OGD). (A–C) Representative images of immunofluorescence staining of (A) FGF7 (red), c-TNT (green) and DAPI (blue), (B) FGF7 (red), vimentin (green) and DAPI (blue) and (C) FGF7 (red), CD34 (green) and DAPI (blue) in the infarct zone of mouse hearts in sham group and 7 days after MI. c-TNT: cardiomyocytes marker. Vimentin: fibroblasts marker. CD34: endothelial cells marker. Scale bar, 50 μ m. (D) Western blotting analysis of FGF7 expression in adult cardiomyocytes (ACMs) and adult cardiac fibroblasts (ACFs) in sham or MI mice. $n = 4$ in per group. (E) Cell lysates of NRCMs were used to detect the FGF7, Bax, Bcl-2 as well as c-Cas-3 protein levels by Western blot and quantified by Image J software. c-Cas-3: cleaved-Caspase-3. $n = 4$ in per group. All values are presented as mean \pm SD. N.S: non-significant, * $P < 0.05$, *** $P < 0.001$. (For interpretation of the references to colour in this figure legend, the reader is referred to the Web version of this article.)

performed according to previous method [35]. Briefly, the cells were cultured in serum/glucose-free medium and exposed to an environment of 1% O_2 for 6 h with or without recombinant FGF7 (150 ng/mL).

For pathway analysis, antagonist: LY294002 (Selleck, 10 μ M) and ML385 (SML1833, Sigma-Aldrich, 30 μ M) and N-acetyl-L-cysteine (NAC, a pharmacological anti-oxidant molecule, Sigma-Aldrich, V900429, 2 mM) were pretreated for 2 h before OGD treatment and FGF7 administration, respectively. BGJ398 (Selleck, 872511-34-7, 1 mM), an inhibitor of FGFR, was applied to inhibit the receptor of FGF7 in NRCMs for 6 h HXK2VBD peptide (Merck, 376816, 100 μ M) was pretreated for 1 h before OGD treatment and FGF7 administration. 3-Bromopyruvate (3-BrPA, Sigma, 16490, 100 μ M) was applied to inhibit the HXK2 expression in NRCMs for 6 h. For H_2O_2 treatment, cells were incubated in the 200 μ M H_2O_2 . The duration of treatment was 6 h.

2.6. Immunofluorescence staining of heart sections and NRCMs

For immunofluorescence staining, heart tissue sections (10 μ m) were incubated with primary antibodies including rabbit anti-c-TNT (Abclonal, A4914; 1: 200), anti-CD34 (Abcam, ab81289; 1: 200), anti-Vimentin (Abcam, ab92547; 1: 200), anti-HXK2 (Proteintech, 22029-1-AP; 1:200) and mouse anti-FGF7 (Santa Cruz Biotechnology, sc-365440; 1: 200), anti-COXIV (Cell Signaling Technology, 11967S; 1:200) for 24 h at 4 $^{\circ}$ C, followed by secondary antibodies including the Alexa Flour 488-conjugated anti-rabbit (Abcam, ab150077; 1: 200) antibody and Alexa Flour 647-conjugated anti-mouse (Abcam, ab150115; 1: 200) antibody for 1 h at room temperature. The nuclei were labeled with 4,6 Diamidino-2-phenylindole (DAPI) for 1 h. In addition, to evaluate Nrf2 nuclear localization *in vivo*, rabbit anti-Nrf2 antibody (Abcam, ab31163; 1: 200) and mouse anti-c-TNT (Huabio, EM1701-39; 1: 200) were used as primary antibodies.

For NRCMs immunofluorescence staining, the cells were fixed in 4%

paraformaldehyde (PFA)/PBS for 10 min, and further immersed in 0.5% Triton for 15 min. NRCMs were incubated with rabbit anti-Nrf2 antibody (Abcam, ab31163; 1: 200), anti-HXK2 (Proteintech, 22029-1-AP; 1:200) and mouse anti-COXIV (Cell Signaling Technology, 11967S; 1:200) overnight at 4 $^{\circ}$ C, followed by the anti-rabbit antibody (conjugated with Alexa Flour 488) and anti-mouse antibody (conjugated with Alexa Flour 647) for 1 h. The nuclei were stained with DAPI for 1 h.

Heart sections and NRCMs were imaged under a confocal microscope (Leica TCS SP8, Germany).

2.7. Statistical analysis

All data were analyzed by using GraphPad Prism 8.0 and were presented as mean \pm SD. Two-tailed Student's t-test (two groups) and one-way analysis of variance (multiple groups) were performed for comparisons. A value of $P < 0.05$ was considered to be statistically significant.

3. Results

3.1. FGF7 is downregulated in cardiomyocytes upon MI and oxygen-glucose deprivation (OGD)

To explore the mechanistic link between FGF7 and cardiac apoptosis following ischemic injury *in vivo*, a mouse model of MI was constructed. The FGF7 level and colocalization of FGF7 and cardiac troponin (c-TNT) were decreased in the infarcted area of mice with MI according to immunofluorescence staining (Fig. 1A). By contrast, colocalization of FGF7 and vimentin was not significantly changed upon MI (Fig. 1B). Furthermore, double immunofluorescence staining of FGF7 and CD34 showed that FGF7 was barely expressed in endothelial cells (Fig. 1C). To verify these results, we extracted cardiomyocytes and fibroblasts from

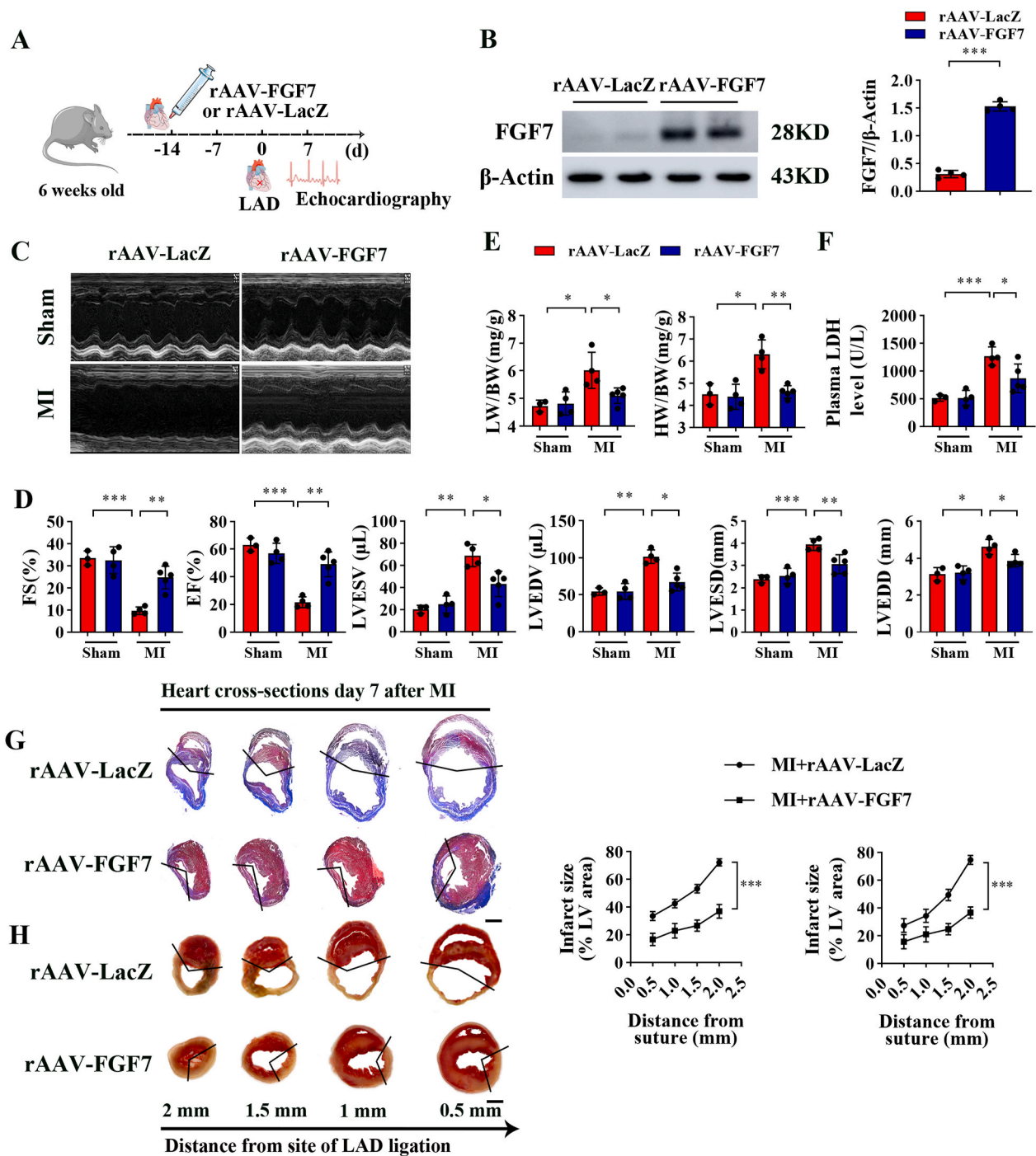


Fig. 2. FGF7 attenuates MI-induced cardiac dysfunction *in vivo*. (A) Experimental procedure for injecting mice with rAAV-FGF7 or rAAV-LacZ. (B) The efficiency of FGF7 overexpression by rAAV-FGF7 was assessed by Western blot and quantified with Image J software. $n = 4$ in per group. (C) Representative M-mode echocardiograms obtained from rAAV-FGF7 injected and rAAV-LacZ injected mice subjected to MI or sham surgery. (D) Echocardiographic measurements of fractional shortening (FS), ejection fraction (EF), left ventricular end-systolic volume (LVESV), left ventricular end-diastolic volume (LVEDV), left ventricular end-systolic diameter (LVESD) and left ventricular end-diastolic diameter (LVEDD) in rAAV-FGF7 injected and rAAV-LacZ injected heart after sham operation or 7 days post-MI. (E) Summarized data of lung weight/body weight (LW/BW), heart weight/body weight (HW/BW) for sham- and MI-operated mice 7 days after surgery. (F) Plasma levels of LDH in rAAV-LacZ or rAAV-FGF7 injected mice after MI. (G–H) Masson trichrome staining (G) and TTC staining (H) of sequential heart cross sections from rAAV-FGF7 or rAAV-LacZ injected mice on day 7 after MI. Scale bar: G&H, 1000 μ m $n = 3$ –5 in per group. All values are presented as mean \pm SD. * $P < 0.05$, ** $P < 0.01$, *** $P < 0.001$.

adult hearts of sham group and mice with MI. Western blotting demonstrated that FGF7 was downregulated in cardiomyocytes, but not in fibroblasts, upon MI (Fig. 1D). Then we verified the above results in primary cultures of neonatal rat cardiomyocytes (NRCMs). As expected, FGF7 level was decreased in the OGD group accompanied by an increase

of apoptosis compared with the control group (Fig. 1E). Overall, these results demonstrate that FGF7 is downregulated in cardiomyocytes upon MI injury.

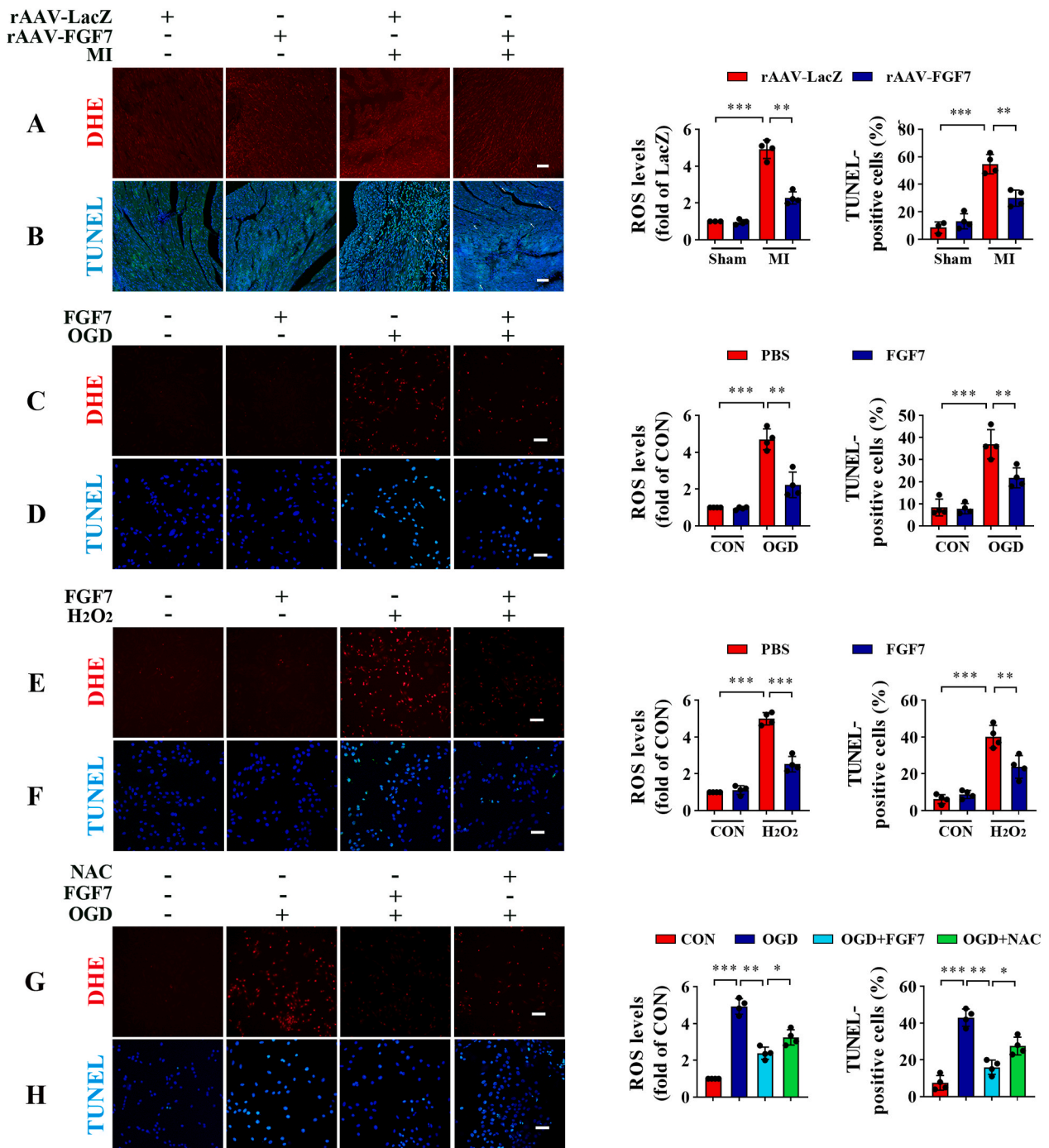


Fig. 3. FGF7 mitigates cardiomyocyte apoptosis by attenuating oxidative stress. (A–B) Representative images of (A) DHE staining and (B) TUNEL staining of heart sections from rAAV-LacZ injected and rAAV-FGF7 injected mice after MI. $n = 3-4$ in per group, Scale bar: A&B, 50 μm . (C–D) Representative images of (C) DHE staining and (D) TUNEL staining of NRCMs treated with or without FGF7 under OGD treatment. Scale bar: C, 100 μm ; D, 50 μm . (E–F) Representative images of (E) DHE staining and (F) TUNEL staining of NRCMs in the presence or absence of FGF7 treated with or without H₂O₂ (200 μM for 6 h). Scale bar: E, 100 μm ; F 50 μm . (G–H) Representative images of (G) DHE staining and (H) TUNEL staining of NRCMs in the presence or absence of FGF7 treated with or without NAC (2 mM pretreated for 2 h) under OGD condition. Scale bar: G, 100 μm ; H, 50 μm $n = 4$ in per group. All values are presented as mean \pm SD. * $P < 0.05$, ** $P < 0.01$, *** $P < 0.001$.

3.2. FGF7 attenuates MI-induced cardiac dysfunction and injury in vivo

To further elucidate the role of FGF7 in cardiomyocyte apoptosis and cardiac function, rAAV-FGF7 was used to overexpress FGF7 in mice prior to MI. Two weeks later, mice underwent permanent left artery ligation (LAD) and were sacrificed after 7 days following echocardiography (Fig. 2A). The efficiency of FGF7 overexpression was determined

by western blotting (Fig. 2B).

To evaluate the potential role of FGF7 in cardiac function under ischemic and hypoxic conditions, echocardiography was performed. Echocardiographic parameters (including fractional shortening and left ventricular (LV) ejection fraction, LV internal diameter, and end-systolic volume at end systole) were significantly improved in FGF7-overexpressing mice compared with LacZ-injected mice after 7 days of

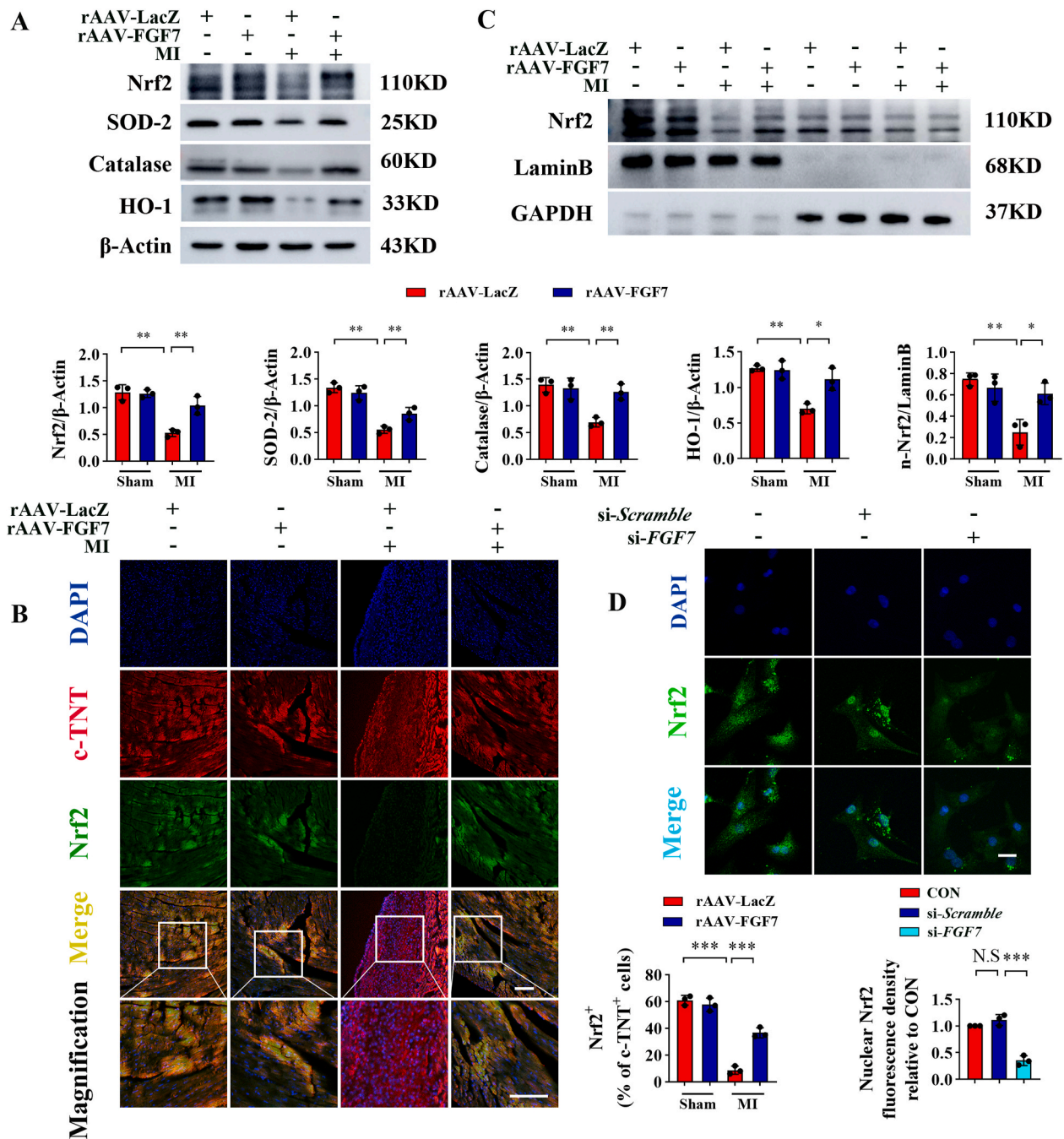
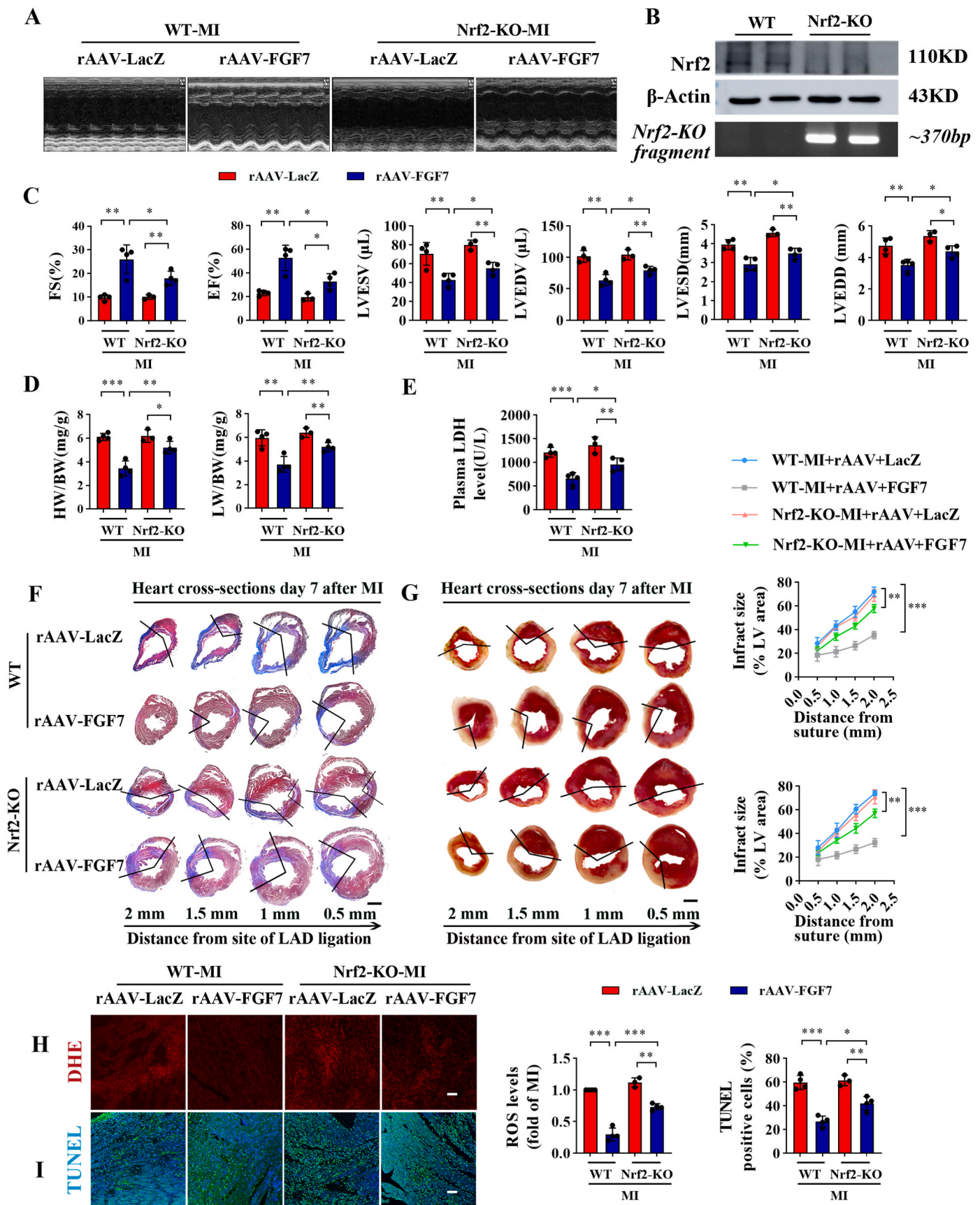


Fig. 4. FGF7 promotes nuclear translocation of Nrf2 to scavenge excess ROS. (A) The protein levels of Nrf2, SOD-2, Catalase and HO-1 in heart tissues of mice injected with rAAV-FGF7 or rAAV-LacZ after MI and assessed by Western blot and quantified by Image J software. (B) Nrf2 nuclear translocation was determined by immunofluorescent staining in rAAV-FGF7 or rAAV-LacZ injected mice after MI. Scale bars: 100 μ m. (C) Nuclear and cytosolic extracts of heart tissues were isolated. Protein levels of Nrf2 in heart tissues injected with rAAV-LacZ or rAAV-FGF7 measured by Western blot and quantified by Image J software. (D) Nrf2 nuclear translocation was determined by immunofluorescent staining in NRCMs transfected with si-Scramble or si-FGF7. The green area represented Nrf2 and the nucleus was blue. Scale bars: 20 μ m n = 3 in per group. All values are presented as mean \pm SD. * P < 0.05, ** P < 0.01, *** P < 0.001. (For interpretation of the references to colour in this figure legend, the reader is referred to the Web version of this article.)

MI (Fig. 2C&D). Morphological analysis indicated that the ratios of lung weight to body weight and heart weight to body weight were higher in LacZ-injected mice than in FGF7-overexpressing mice after 7 days of MI (Fig. 2E). These findings suggest that cardiac remodeling, pulmonary edema, and heart failure are attenuated in FGF7-overexpressing mice subjected to MI.

Furthermore, MI- or OGD-induced cardiomyocyte apoptosis, as demonstrated by the increased the ratio of Bax/Bcl-2 and the level of cleaved-Caspase-3, was alleviated by FGF7 overexpression

(Fig. S1A&B). Double immunofluorescence staining of cleaved-Caspase-3 and c-TNT showed that FGF7 overexpression significantly attenuated MI-induced cardiomyocyte apoptosis (Fig. S1C). Plasma levels of lactate dehydrogenase (LDH) indicated that the level of cell death was lower in FGF7-overexpressing mice than in LacZ-injected mice after MI (Fig. 2F). Masson's trichrome and TTC staining of serial cross-sections of heart that were cut above the level of ligature and 0.5, 1.0, 1.5, and 2.0 mm below the ligation site demonstrated a modest reduction in infarct size in FGF7-overexpressing mice at day 7 after MI (Fig. 2G&H). To further



(caption on next page)

Fig. 5. Knockout (KO) or inhibition of Nrf2 impairs the cardioprotective effect of FGF7 *in vivo* and *in vitro*. FGF7 overexpression adeno-associated virus (rAAV-FGF7) and control vector (rAAV-LacZ) were injected of 6 weeks old male WT mice and Nrf2-KO mice respectively, two weeks after the injection, these mice were subjected to Sham or LAD operation for 7 days. **(A)** Representative M-mode echocardiograms obtained from wild-type (WT) and Nrf2-KO mice which inject rAAV-LacZ or rAAV-FGF7 subjected to MI or sham surgery. **(B)** The efficiency of Nrf2-KO was assessed by Western blot and PCR analysis. Western blot results quantified with Image J software. **(C)** Echocardiographic measurements of fractional shortening (FS), ejection fraction (EF), left ventricular end-systolic volume (LVESV), left ventricular end-diastolic volume (LVEDV), left ventricular end-systolic diameter (LVESD) and left ventricular end-diastolic diameter (LVEDD) and in wild-type (WT) and Nrf2-KO mice which inject rAAV-LacZ or rAAV-FGF7 after sham operation or 7 days post-MI. **(D)** Summarized data of heart weight/body weight (HW/BW), lung weight/body weight (LW/BW) for WT and Nrf2-KO mice. **(E)** Plasma levels of LDH in WT and Nrf2-KO mice. **(F–G)** Masson trichrome staining **(F)** and TTC staining **(G)** of sequential heart cross sections from WT or Nrf2-KO mice. Scale bar: E&F, 1000 μm . **(H–I)** Representative images of **(H)** DHE staining and **(I)** TUNEL staining of heart sections from WT or Nrf2-KO mice injected with rAAV-LacZ or rAAV-FGF7 after MI. Scale bar: H&I, 50 μm n = 3–4 per group. All values are presented as mean \pm SD. *P < 0.05, **P < 0.01, ***P < 0.001.

elucidate the important role of FGF7 in cardiomyocyte apoptosis, FGF7-targeting small interfering RNA (si-FGF7) was used to inhibit FGF7 expression in NRCMs prior to OGD. The increased ratio of Bax/Bcl-2 and level of cleaved-Caspase-3 indicated that silencing of FGF7 aggravated cardiomyocyte apoptosis (Fig. S2A). TUNEL staining of NRCMs further demonstrated that silencing of FGF7 promoted cardiomyocyte apoptosis upon OGD treatment (Fig. S2B). To determine whether the effect of FGF7 was receptor-mediated, cardiomyocytes were treated with an FGFR antagonist, BGJ398 (BGJ). As expected, BGJ abolished the cardioprotective effects of FGF7, as assessed by elevations of the percentage of TUNEL-positive cells, ratio of Bax/Bcl-2, and level of cleaved-Caspase-3 (Fig. S2C&D), which indicated that FGF7 attenuates OGD-induced NRCM apoptosis via FGFRs. Together, these findings suggest that overexpression of FGF7 attenuates MI-caused cardiomyocyte apoptosis and improves heart function after MI.

3.3. FGF7 mitigates cardiomyocyte apoptosis by attenuating oxidative stress

ROS play an essential role in apoptosis, and FGF7 restrains apoptosis by alleviating oxidative stress [6,36]. Therefore, we explored whether FGF7 mitigates cardiac apoptosis by attenuating oxidative stress. We first investigated the roles of FGF7 on regulation of oxidative stress in mouse myocardial tissues after MI. MI rapidly induced generation of ROS in mouse hearts accompanied by severe cell death, as evidenced by the increased intensities of dihydroethidium (DHE) fluorescence and TUNEL, respectively (Fig. 3A&B), together with accumulation of the oxidation product 3-nitrotyrosine (3-NT) (Fig. S3A) and elevation of the lipid peroxidation (LPO) level (Fig. S3B). However, FGF7 overexpression suppressed MI induced oxidative stress and apoptosis. Similarly, FGF7 inhibited oxidative stress and mitigated apoptosis in NRCMs upon OGD treatment (Fig. S2B, Fig. 3C&D, and Fig. S3C&D).

We then treated NRCMs with H₂O₂. The increase in DHE fluorescence intensity and TUNEL-positive cells (Fig. 3E&F), accumulation of 3-NT (Fig. S3E), and elevations of the ratio of Bax/Bcl-2 ratio and cleaved-Caspase-3 level (Fig. S3F) were significantly alleviated by cotreatment with FGF7. Meanwhile, the increase of ROS levels, as demonstrated by DHE fluorescence and 3-NT immunoblotting, was restrained by N-acetyl cysteine (NAC) or FGF7 treatment (Fig. 3G and Fig. S3G). Consistently, NAC or FGF7 treatment also reduced the elevations of apoptotic cells, ratio of Bax/Bcl-2, and cleaved-Caspase-3 level (Fig. 3H and Fig. S3H). Together, these results indicate that FGF7 exerts its antiapoptotic function by inhibiting oxidative stress, and that its antioxidant activity is comparable with or greater than that of NAC, a well-known antioxidant.

3.4. FGF7 promotes nuclear translocation of Nrf2 to scavenge excess ROS

Nrf2 is an important regulator of the antioxidant system in many heart diseases, including MI [17,37]. To further explore whether FGF7 elicits antioxidative effects by activating the Nrf2 signaling upon MI, we first examined the proteins levels of Nrf2 signaling-related proteins by western blotting. OGD treatment decreased the protein levels of Nrf2 and its downstream antioxidant proteins, including Catalase, HO-1, and SOD-2. These effects were reversed by FGF7 administration (Fig. S4A),

consistent with the results obtained *in vivo* (Fig. 4A). In parallel, OGD treatment significantly decreased the mRNA levels of Nrf2 and its target genes (*HO-1*, *NQO1*, *NQO2*, *SOD-2*, and *Catalase*), and these effects were reversed by FGF7 administration (Fig. S4B). Immunofluorescence analysis suggested that FGF7 promoted Nrf2 nuclear translocation upon OGD treatment (Fig. S4C). The results of Western blot analysis of nuclear extracts from NRCMs were consistent with the immunofluorescence staining results (Fig. S4D). Immunofluorescence staining of Nrf2 and c-TNT in heart tissue sections indicated that the protein level and Nrf2 nuclear accumulation were significantly decreased in cardiomyocytes after MI, while FGF7 overexpression promoted nuclear accumulation of Nrf2 compared with LacZ-injected mice (Fig. 4B). Western blot analysis of nuclear extracts from heart tissues yielded similar findings (Fig. 4C), while si-FGF7 treatment significantly decreased nuclear accumulation of Nrf2 (Fig. 4D). Together, these results indicate that FGF7 increases the protein level and nuclear accumulation of Nrf2 upon MI and OGD treatment.

3.5. Knockout (KO) or inhibition of Nrf2 partially impairs the cardioprotective effect of FGF7 *in vivo* and *in vitro*

FGF7 induced activation of Nrf2 upon MI, and Nrf2 is an important regulator of heart injury upon MI [38–40]. Therefore, we further explore the potential role of Nrf2 in cardiac apoptosis and function, and explored whether the protective effects of FGF7 against MI are dependent on Nrf2. Nrf2-KO and WT mice with or without overexpression of FGF7 were subjected to MI. The efficiency of Nrf2-KO was determined by PCR and western blotting (Fig. 5B). To determine the Nrf2 role in MI, Nrf2-KO and WT mice (8 weeks) were subjected to LAD ligation. Echocardiography analysis revealed that cardiac dysfunction after MI was significantly improved in FGF7-overexpressing WT mice compared with WT mice, and this improvement was partially abolished in Nrf2-KO mice (Fig. 5A&C). The results of morphological analysis and measurements of plasma LDH levels and infarct sizes were consistent with the echocardiographic results (Fig. 5D–G). Consistently, the protective effects of FGF7 were partially abolished in Nrf2-KO mice, as demonstrated by higher levels of ROS and apoptosis compared with FGF7-overexpressing WT mice (Fig. 5H&I and Fig. S5A). In addition, ML385 (an inhibitor of Nrf2) partly blocked the protective effect of FGF7 in NRCMs upon OGD treatment (Fig. S5B), with increases of the DHE fluorescence intensity and TUNEL-positive cells (Fig. S5C&D). The ratio of Bax/Bcl-2 and levels of cleaved-Caspase-3 and 3-NT were increased in the presence of ML385 upon OGD treatment (Fig. S5E&F). Meanwhile, the levels of downstream of Nrf2 (Catalase and SOD-2) were also decreased in the presence of ML385 (Fig. S5E). Together, these results reveal that the cardioprotective effect of FGF7 is partially abolished by KO or inhibition of Nrf2.

3.6. FGF7 promotes nuclear translocation of Nrf2 via PI3K α /AKT signaling during MI

Given that AKT is a crucial upstream mediator of Nrf2, and that FGF7 induces AKT phosphorylation, we therefore hypothesized that FGF7 activates Nrf2 via PI3K α /AKT pathway upon MI injury. To verify this

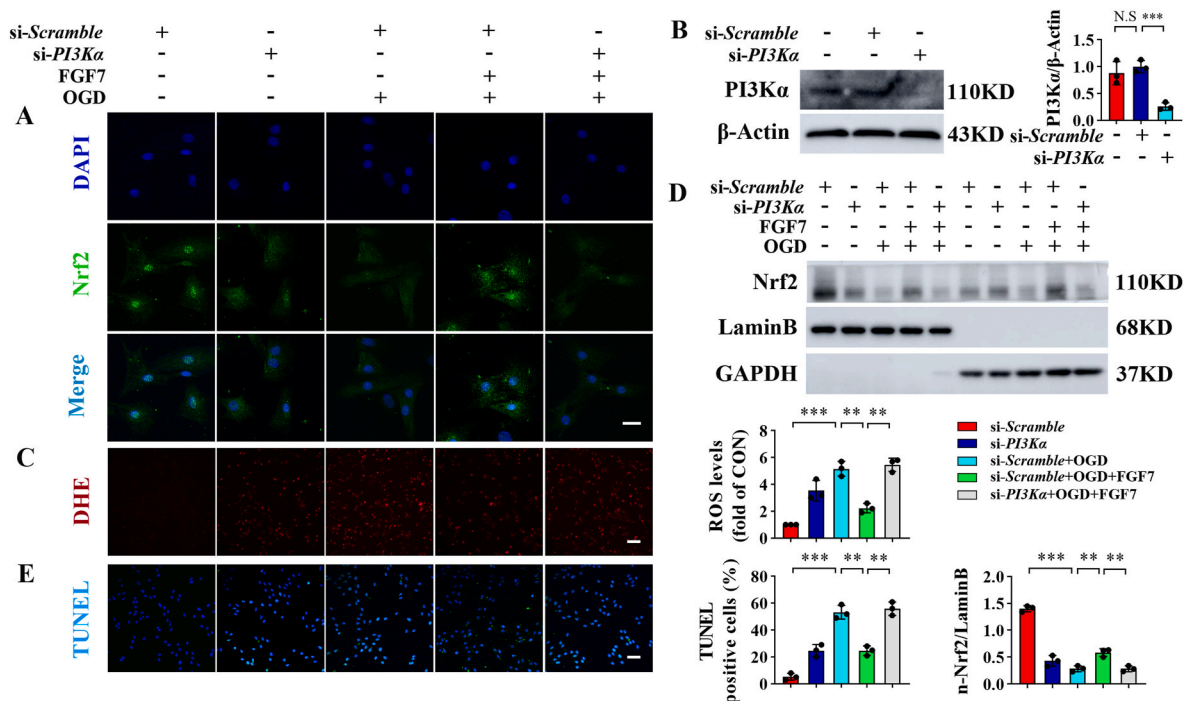


Fig. 6. FGF7 promotes nuclear translocation of Nrf2 via PI3K α /AKT signaling during MI. (A) Nrf2 nuclear translocation was determined by immunofluorescent staining in NRCMs transfected with si-Scramble or si-PI3K α . The green area represented Nrf2 and the nucleus was blue. Scale bars: 20 μ m. (B) The efficiency of si-PI3K α was assessed by Western blot analysis. Western blot results quantified with Image J software. (C) Images of DHE staining in NRCMs. Scale bars: 100 μ m. (D) Nuclear and cytosolic extracts of NRCMs were isolated. Protein levels of Nrf2 in NRCMs transfected with si-Scramble or si-PI3K α measured by Western blot and quantified by Image J software. (E) Images of TUNEL staining in NRCMs. Scale bars: 50 μ m n = 3 in per group. All values are presented as mean \pm SD. **P < 0.01, ***P < 0.001. (For interpretation of the references to colour in this figure legend, the reader is referred to the Web version of this article.)

hypothesis, PI3K α -targeting small interfering RNA (si-PI3K α) was utilized to inhibit PI3K α /AKT signaling in NRCMs prior to OGD treatment. The efficiency of si-PI3K α was determined by western blotting (Fig. 6B). Double immunofluorescence staining of Nrf2 and DAPI showed that FGF7 promoted nuclear accumulation of Nrf2 upon OGD treatment, but this effect was reversed by si-PI3K α (Fig. 6A). Moreover, DHE staining and TUNEL showed that the levels of ROS and apoptotic cells upon OGD treatment were decreased by FGF7 administration, but these effects were reversed in the presence of si-PI3K α (Fig. 6C&E). Western blot analysis of Nrf2 from nuclear extracts in NRCMs yielded consistent results as immunofluorescence staining in the presence of si-PI3K α upon OGD treatment (Fig. 6D).

Moreover, pretreatment with the PI3K inhibitor LY294002 largely reversed the promotion of Nrf2 nuclear translocation by FGF7, as indicated by colocalization analysis of Nrf2 and DAPI immunofluorescence staining and western blotting of nuclear extracts (Fig. S6A&B). Furthermore, pretreatment with LY294002 abolished the antioxidative and antiapoptotic effects of FGF7 upon OGD treatment, as indicated by DHE staining and TUNEL (Fig. S6C&D). In addition, the level of 3-NT was upregulated in the presence of LY294002 compared with FGF7 treatment upon OGD treatment (Fig. S6E). Meanwhile, LY294002 largely impaired activation of AKT signaling and upregulation of the Nrf2 protein level by FGF7 in NRCMs upon OGD treatment (Fig. S6F). Moreover, AKT inhibition abolished downregulation of the ratio of Bax/Bcl-2 and cleaved-Caspase-3 level by FGF7 after OGD treatment (Fig. S6F). Together, these results reveal that FGF7 activates Nrf2 by PI3K α /AKT pathway and thereby protects the heart against MI injury.

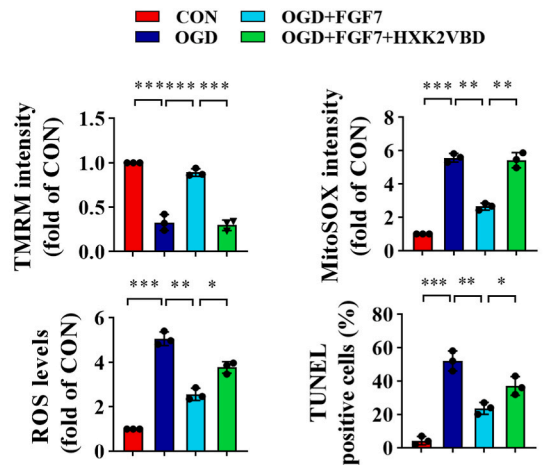
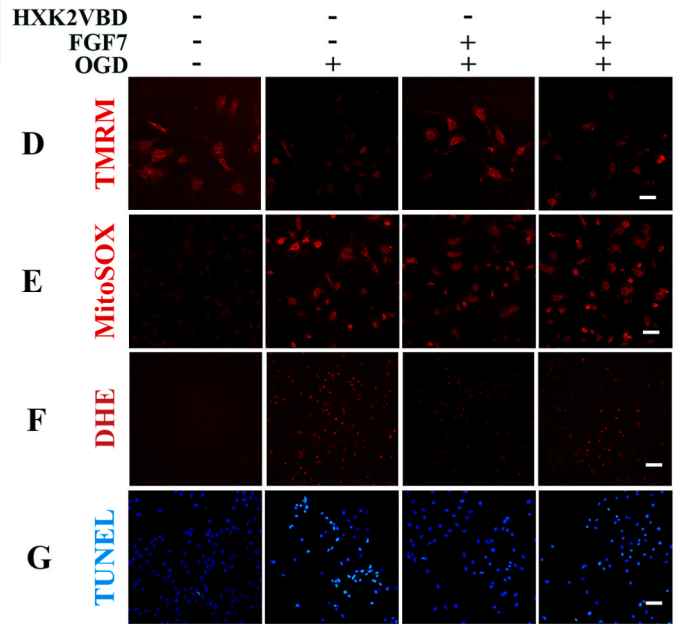
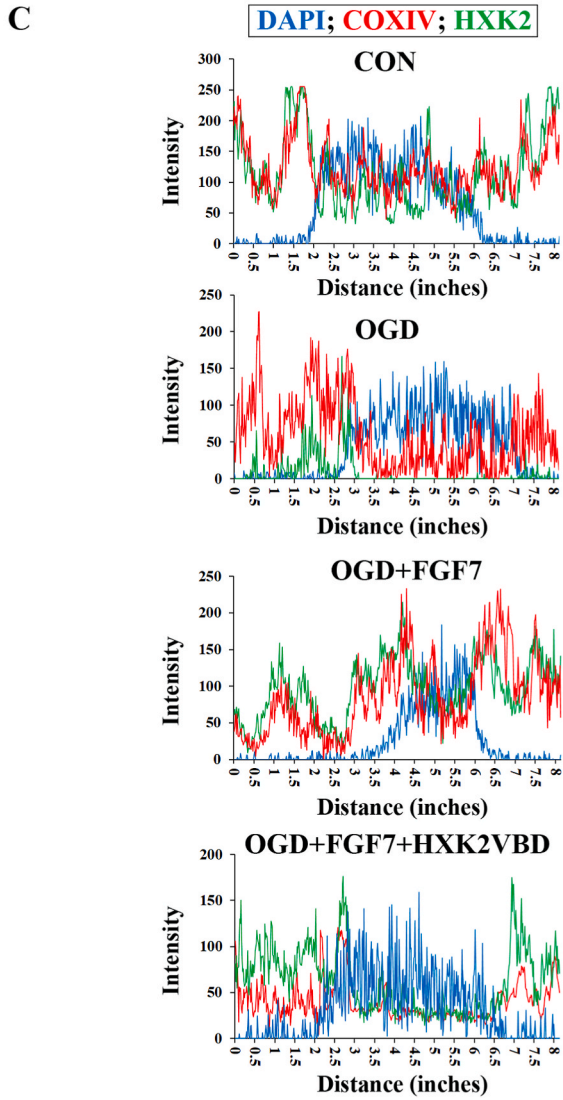
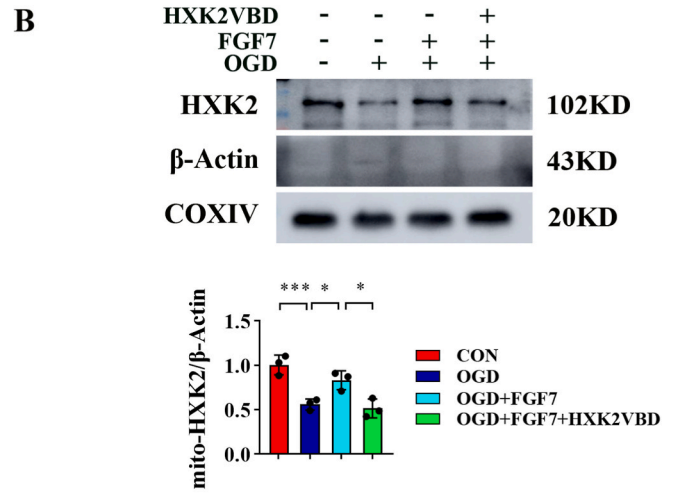
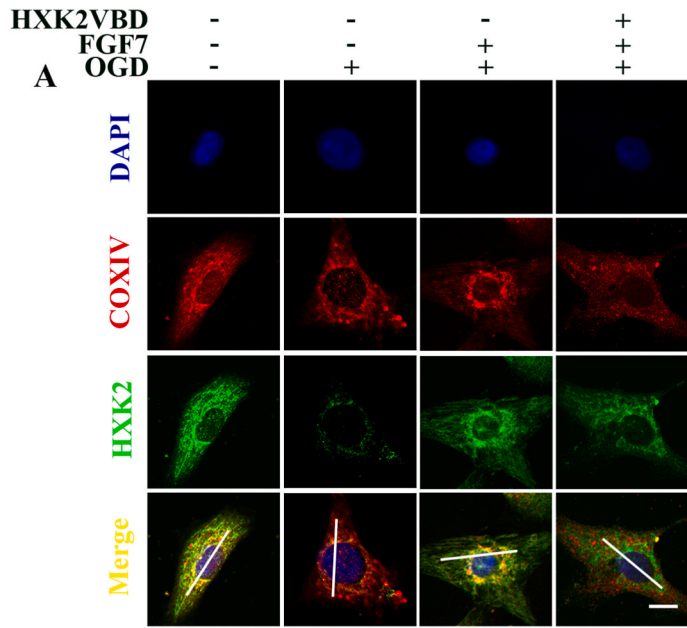
3.7. FGF7 promotes mitochondrial localization of HXK2 to protect against superoxide injury

Considering that KO of Nrf2 only partially reversed the protective effect of FGF7 (Fig. 5), while inhibition of AKT abolished the

antioxidative and antiapoptotic effects of FGF7 in NRCMs, we speculate that FGF7-AKT exert their cardioprotective effects through Nrf2 and other factors. Increased expression of HXK2 promote the coupling between HXK2 and mitochondria, which protects cells against mitochondrial oxidative stress [21,41,42]. AKT is an important upstream regulator of HXK2 and maintains mitochondrial homeostasis by promoting mitochondrial localization of HXK2 [23]. Therefore, we hypothesized that FGF7-AKT promote mitochondrial localization of HXK2 to elicit antioxidative and antiapoptotic effects. To investigate the function of HXK2 in FGF7-mediated heart protection, we explored the role of FGF7 in regulation localization of HXK2 in mitochondria. FGF7 promoted mitochondrial localization of HXK2, as indicated by an increased level of HXK2 in mitochondria (Fig. 7B) and increased co-staining of HXK2 puncta (green) and COX IV (red) (Fig. 7A&C). These effects were reversed in the presence of HXK2VBD, a HXK2 competitive inhibitory peptide. HXK2VBD counteracted the cardioprotective effects of FGF7 to some extent, as demonstrated by increases of mitochondrial depolarization (Fig. 7D and Fig. S7A), superoxide production (Fig. 7E), ROS level in NRCMs (Fig. 7F), and TUNEL-positive NRCMs (Fig. 7G). In addition, the HXK2 inhibitor 3-BrPA partly abrogated the beneficial effects of FGF7 in NRCMs subjected to OGD treatment, as determined by increases of the Bax/Bcl-2 ratio and protein level of cleaved-Caspase-3 (Fig. S7B). Together, these results reveal that FGF7 promotes mitochondrial localization of HXK2 to protect against superoxide injury upon OGD treatment.

3.8. FGF7 promotes mitochondrial localization of HXK2 via AKT to protect against oxidative stress in vivo and in vitro

AKT phosphorylates HXK2, which increases mitochondrial association of HXK2 to protect cardiomyocytes against apoptosis, and this function is independent of its enzymatic activity [23,41]. We debate whether FGF7 promotes mitochondrial localization of HXK2 via AKT.



(caption on next page)

Fig. 7. FGF7 promotes mitochondrial localization of HXK2 to protect against superoxide injury. HXK2VBD, which inhibits mitochondrial localization of HXK2, were pretreated for 1 h before OGD treatment and FGF7 administration in NRCMs. **(A)** Representative immunofluorescence analysis of HXK2 (green) in NRCMs. The COX IV immunostaining (red) highlights mitochondria, and nuclei were stained with DAPI (blue), scale bars: 10 μ m. **(B)** Mitochondrial was isolated to detect the HXK2 protein levels in NRCMs. COX IV and β -Actin were served as loading controls for mitochondrial. **(C)** White lines in merged images **(A)** indicate the area where the distances between HXK2, COX IV, and DAPI were analyzed using ImageJ. **(D)** Mitochondrial membrane potential was detected by TMRM fluorescence staining, scale bars: 25 μ m. **(E)** mtROS of NRCMs was detected by MitoSOX staining assay, scale bars: 50 μ m. **(F–G)** Representative images of **(F)** DHE staining and **(G)** TUNEL staining of NRCMs. Scale bar: **F**, 100 μ m; **G**, 50 μ m $n = 3$ in per group. mtROS: mitochondrial reactive oxygen species. All values are presented as mean \pm SD. * $P < 0.05$, ** $P < 0.01$, *** $P < 0.001$.

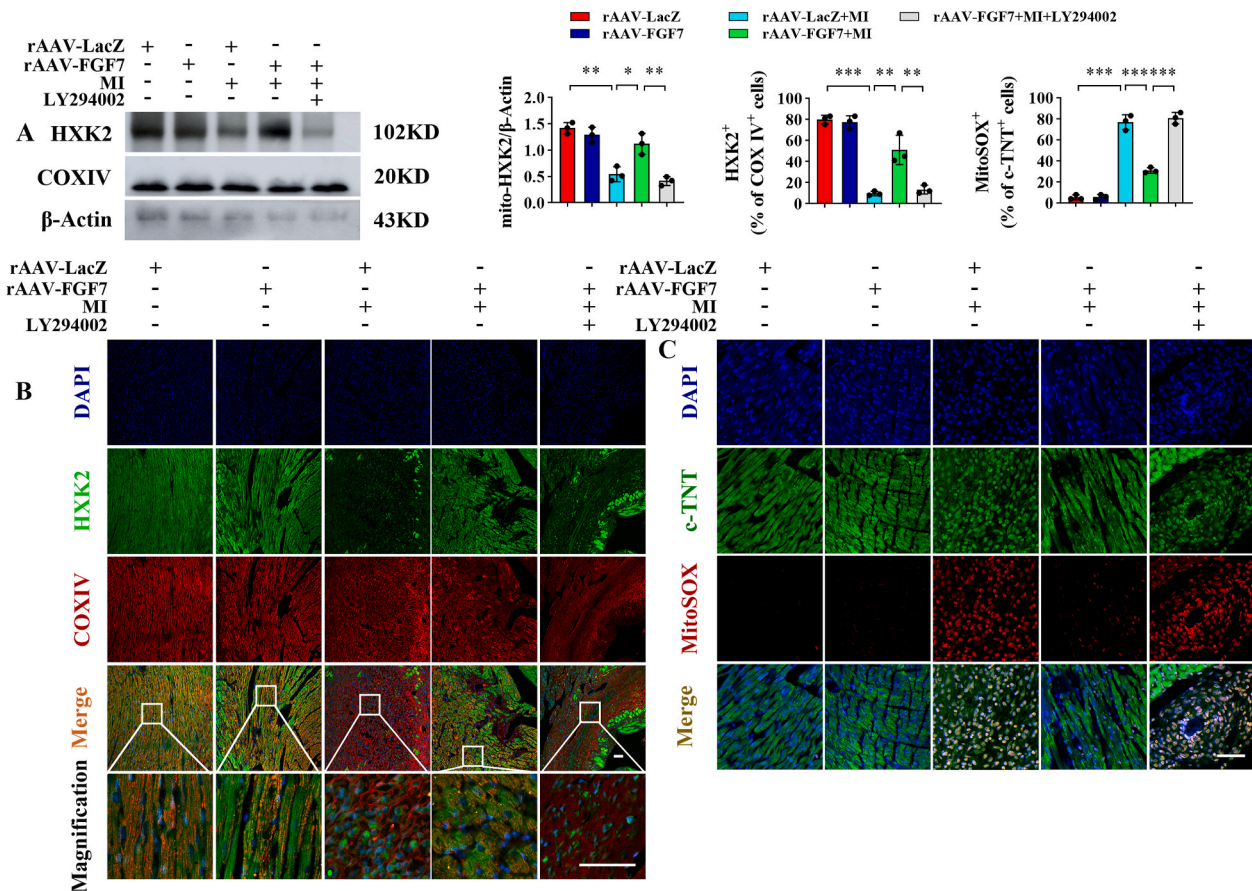


Fig. 8. FGF7 promotes mitochondrial localization of HXK2 via AKT to protect against oxidative stress *in vivo* and *in vitro*. **(A)** Mitochondrial was isolated to detect the HXK2 protein levels in heart tissue sections. COX IV and β -Actin were served as loading controls for mitochondrial. **(B)** Representative immunofluorescence analysis of HXK2 (green) in heart tissue sections. The COX IV immunostaining (red) highlights mitochondria, and nuclei were stained with DAPI (blue), scale bars: 50 μ m. **(C)** mtROS of heart tissue sections was detected by MitoSOX staining assay, scale bars: 50 μ m $n = 3$ in per group. All values are presented as mean \pm SD. * $P < 0.05$, ** $P < 0.01$, *** $P < 0.001$. (For interpretation of the references to colour in this figure legend, the reader is referred to the Web version of this article.)

FGF7 restored MI-downregulated the expression of HXK2 and promoted mitochondrial localization of HXK2, as demonstrated by increased mitochondrial binding of HXK2 (Fig. 8A). Double immunofluorescence staining of HXK2 (green) and COX IV (red) showed that FGF7 increased mitochondrial localization of HXK2, and this effect was blocked by pretreatment with LY294002 (Fig. 8B). Furthermore, LY294002 abrogated the antioxidant effects of FGF7 *in vivo*, as determined by upregulated superoxide generation in cardiomyocytes after MI (Fig. 8C). In the presence of si-PI3K α , the mitochondrial localization of HXK2 was decreased compared with that observed following FGF7 administration upon OGD treatment (Fig. S8A). Immunofluorescence analysis of HXK2 and COX IV indicated that inhibition of PI3K α /AKT signaling decreased the mitochondrial localization of HXK2 (Fig. S8B&C). Furthermore, si-PI3K α largely reversed the antioxidant effects of FGF7, as demonstrated by increased mitochondrial depolarization (Fig. S8D) and superoxide generation (Fig. S8E). These results indicate that FGF7 promotes mitochondrial localization of HXK2 via PI3K α /AKT signaling to protect against OGD-induced injury. In the presence of HXK2VBD and

ML385, the cardioprotective effects of FGF7 were largely abolished, as determined by increases of the ratio of Bax/Bcl-2 and level of cleaved-Caspase-3 (Fig. S9A). Meanwhile, DHE staining showed that HXK2VBD and ML385 treatment increased the ROS levels (Fig. S9B). Together, these findings demonstrate that Nrf2 and HXK2 are both critical for the protective effects of FGF7 against MI injury.

4. Discussion

Cardiomyocyte apoptosis is an important hallmark of MI [43,44]. Increased oxidative stress due to MI causes apoptosis, which is an important pathogenic mechanism underlying myocardial ischemia-associated complications, including fibrosis and adverse cardiovascular outcomes [6]. ROS are considered as a double-edged sword. Low levels of ROS have multiple functions in various physiological processes, such as gene expression, the immune response, and cellular homeostasis maintenance [45]. By contrast, high levels of ROS elicit pathological effects and damage components of cellular,

including nucleic acids, proteins, and lipids [46]. Excessive accumulation of ROS is defined as oxidative stress, which is a key mediator of cell death [47]. Therefore, ROS homeostasis must be strictly regulated to maintain cell health, and its disruption is considered a major cause of myocardial injury [48]. In addition, ROS-induced mitochondrial insults lead to greater ROS accumulation, which results in more severe mitochondrial damage and cell death [49].

Nrf2 is a vital mediator of the oxidative stress and increases expression of antioxidants to eliminate ROS. Accordingly, expression of its downstream targets, SOD-2 and Catalase, was decreased in heart tissue of Nrf2-KO mice (Fig. S5A). Nrf2 alleviates cardiac damage upon ischemic injury, and the Nrf2-KO heart is more susceptible to MI [19, 38–40]. In this study, we confirmed that MI injury decreases the Nrf2 level and increases ROS accumulation in cardiomyocytes, consistent with previous studies. Traditionally, researchers have tried to reverse oxidative stress injury by activating Nrf2 signaling to scavenge accumulated ROS. However, protection against oxidative stress by Nrf2 is potentially limited because ROS are continually produced after injury [50]. Inhibiting overproduction and release of ROS is also an important strategy to alleviate oxidative stress-induced injury.

HXXK2 is a rate-limiting enzyme in glycolysis and localizes to mitochondria [21]. It modulates energy production and mitochondrial superoxide generation [51–53]. HXXK2 suppresses cell death by inhibiting formation of mitochondrial permeability transition pores, which is related to VDAC protein [22]. HXXK2 deficiency exaggerates cardiac hypertrophy by increasing ROS production [54]. Furthermore, phosphorylation at Thr-473 promotes binding of HXXK2 to mitochondria and protects cardiomyocytes against ROS [23]. Our laboratory also demonstrated that HXXK2 is critical for alleviating generation of mitochondrial superoxide by translocating from the cytosol to mitochondria in a type 2 diabetes mouse model after acidic FGF stimulation [55]. In this study, mitochondrial translocation of HXXK2 was reduced in MI stimulation accompanied by enhancement of oxidative stress, indicating that mitochondrial localization of HXXK2 is closely related to steady-state maintenance of mitochondrial homeostasis, and thereby reduces ROS production and cell injury. Furthermore, the level of HXXK2 was decreased in response to oxidative injury, consistent with previous reports [56]. The aforementioned findings suggest that suppression of ROS production by activation of HXXK2 is a potential antioxidative strategy. However, it is difficult to restore redox homeostasis by alleviating production of ROS without increasing scavenging of ROS [57]. Therefore, regulation of both formation and scavenging of ROS may be an effective strategy to treat MI-induced oxidative injury. However, few regulators with such dual functions have been identified.

FGF7, known as keratinocyte growth factor, is an important mitogen for regulating growth and division of epithelial cells [58]. It is mainly expressed in smooth muscle, the heart, and the forebrain [11,59]. FGF7 plays pivotal roles in protection against ischemic injury upon flap injury, in the brain, and especially in the kidneys [59–63]. Recombinant FGF7 is used to treat chemoradiation-induced oral mucositis [64]. Importantly, FGF7 is considered to reduce oxidative stress by inducing expression of antioxidative genes [54,65]. These studies indicate that FGF7 negatively regulates oxidative stress. Furthermore, FGF7 is highly expressed in the myocardium during development [66,67]. Taken together, these reports suggest that FGF7 plays crucial roles in myocardial injury, which might be related to regulation of oxidative stress.

To confirm this idea, we investigated expression of FGF7 in heart tissue upon MI and found that it was decreased in cardiomyocytes. Subsequent experiments revealed that overexpression of FGF7 in mice significantly improved cardiac function after MI and reduced myocardial apoptosis, accompanied by attenuation of oxidative stress. These results were verified by exposing NRCMs to OGD in the presence or absence of FGF7. The present study provides the first evidence that FGF7 is an important factor for amelioration of heart injury after MI.

In view of the antioxidative function of FGF7, we speculated that its beneficial effect is closely related with oxidative stress [11,66,67].

Accordingly, we revealed that overexpression of FGF7 restored both the total and nuclear Nrf2 protein levels, accompanied by reductions of oxidative stress and apoptosis. Interestingly, the antioxidant effect of FGF7 upon MI injury was partly abolished in Nrf2-KO mice, indicating the probability that other regulator(s) is involved in the cardioprotective effect of FGF7 following MI injury. NAC, a scavenger of ROS, has potent antioxidative and antiapoptotic activities [68]. The antioxidant effect of NAC was slightly weaker than that of FGF7. This result reinforced our hypothesis that an additional factor(s) is involved in the antioxidant effect of FGF7.

Redox homeostasis is mainly disturbed by enhancement of ROS production and attenuation of ROS elimination [69]. Therefore, we further speculated that the cardioprotective effect of FGF7 is not only dependent on scavenging of ROS mediated by Nrf2 but also on attenuation of ROS generation. HXXK2 is beneficial for maintaining mitochondrial homeostasis and reducing ROS production and cell death [23,24]. It is also a downstream target of FGFs [70]. Therefore, we next investigated whether HXXK2 is another downstream element that mediates the protective functions of FGF7 against oxidative damage. FGF7 administration significantly increased the mitochondrial localization of HXXK2 and subsequently attenuated mitochondrial ROS production upon OGD treatment. The function of HXXK2 in FGF7-mediated alleviation of ROS generation and myocardial protection was confirmed using a competitive inhibitory peptide, HXXK2VBD, which inhibits HXXK2 located in the mitochondria. In the presence of competitive peptide HXXK2VBD, the antioxidant effect of FGF7 was only partially abolished. By contrast, the cardioprotective effect of FGF7 was largely abolished in the presence of both HXXK2VBD and ML385. We predicted that FGF7 elicits antioxidant effects upon MI mainly through both Nrf2 and HXXK2.

PI3K α /AKT signaling plays crucial roles in the pathological process of MI [71–73]. PI3K α regulates multiple downstream pathways that control cell growth, survival, and proliferation. Inhibition of PI3K α by BYL719 worsens cardiac remodeling after MI [71]. AKT activation is required for some therapeutic approaches upon heart ischemic injury [72,73]. In our study, in addition to promoting nuclear translocation of Nrf2, FGF7 increased Nrf2 expression, while inhibition of PI3K α /AKT blocked the effects of FGF7. Thus, we speculated that FGF7 promotes expression of Nrf2 through AKT. In addition, it has been previously reported that Glycogen Synthase Kinase 3 β (GSK3 β) phosphorylates Nrf2, and the phosphorylation induces ubiquitination and therefore degradation of Nrf2 [74]. GSK3 β is inhibited as a downstream target of PI3K/AKT. Mechanistically, PI3K activates AKT by phosphorylation, which in turn phosphorylates and inhibits GSK3 β [74]. This cascade results in inhibition of Nrf2 degradation and promotion of its nuclear translocation. Furthermore, AKT phosphorylates HXXK2 at Thr-473, leading to enhanced binding of HXXK2 to mitochondria and resistance to oxidative injury in cardiomyocytes [23]. However, it is unclear whether PI3K α /AKT simultaneously regulate the functions of Nrf2 and HXXK2 in heart hypoxia/ischemia models. Our results confirmed that FGF7 activates PI3K α /AKT signaling, which is accompanied by increased activation of Nrf2 and HXXK2 together with corresponding decreases in oxidative injury and cell death. By contrast, pharmacological inhibition of PI3K α /AKT reversed the activation of Nrf2 and HXXK2 by FGF7 in an OGD model, and largely abolished the antioxidant effects of FGF7. These results demonstrate that PI3K α /AKT play a critical role in FGF7-mediated cardio protection upon MI.

This study has some limitations. First, FGF7 is also expressed in fibroblasts, and although there was no significant change in FGF7 expression in fibroblasts upon MI injury, it is worth exploring the potential role of FGF7 in fibroblasts. Second, FGF7 is a paracrine factor and is therefore expected to signal via crosstalk between the cardiomyocytes and other cell types. Future studies should investigate the potential functions of FGF7 in intercellular communication. Third, although Nrf2-KO mice have been used to study myocardial oxidative damage, cardiomyocyte-specific knockdown of Nrf2 would more precisely demonstrate its regulatory role in FGF7-mediated protection of

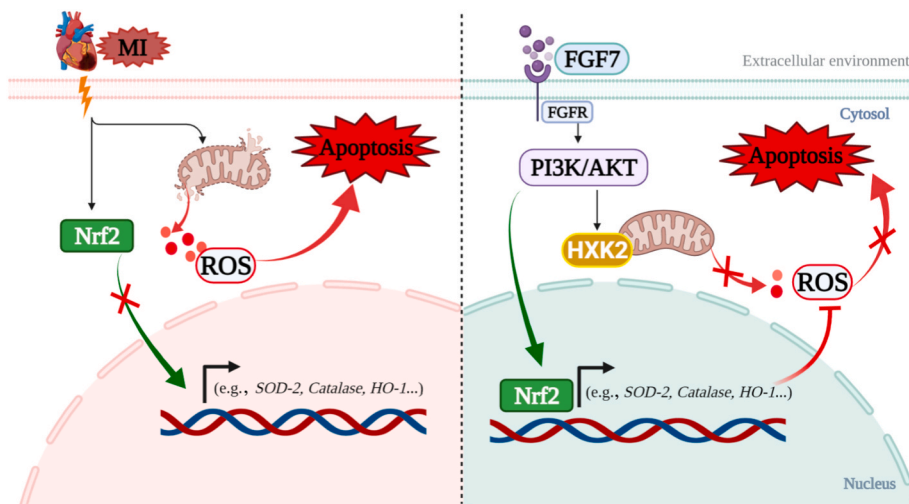


Fig. 9. Schematic illustrating the effects of FGF7 alleviates myocardial infarction by decreasing oxidative stress via PI3K α /AKT mediated regulation of Nrf2 and HXK2. In the condition of myocardial infarction, the function of mitochondrial was disrupted, and produces large amounts of ROS to cause cell apoptosis. FGF7 attenuated myocardial infarction via promoting Nrf2 nuclear translocation and mitochondrial HXK2 localization via PI3K α /AKT signaling pathway to scavenge excessive ROS and inhibit the production of ROS to against cell apoptosis ultimately.

the heart.

Overall, in the present study, we showed that FGF7 significantly preserves heart function after MI by activating PI3K α /AKT signaling to promote nuclear translocation of Nrf2 and mitochondrial localization of HXK2, and thereby maintain the cellular redox balance (Fig. 9).

5. Conclusion

Our data demonstrated that FGF7 protects against MI-induced cardiomyocyte apoptosis for the first time. Mechanistic studies showed that FGF7 overexpression/treatment promoted activation of Nrf2 to increase the elimination of oxidants as well as mitochondrial localization of HXK2 to reduce the production of oxidants in a PI3K α /AKT-dependent manner, thereby alleviating oxidative stress and eventually cardiomyocyte apoptosis. These findings improve understanding of the protective role of FGF7 against MI and could help to develop new pharmacological interventions for cardiovascular disease.

Ethics statement

Animal use and care protocol was approved by the Animals Use and Care Committee of the Wenzhou Medical University, Wenzhou, China.

Funding statement

This work was supported by the National Nature Science Foundation of China (82170365, 82070507 and 81870209), the Zhejiang Provincial Natural Science Foundation (LY19H020005 and LY21H020009), Zhejiang Province Medical and Health Science Program (2019KY099), Wenzhou Science and Technology Bureau Foundation (Y2020180).

Author contribution statement

Lin Mei, Yunjie Chen, Xu Wang, Weitao Cong and Litai Jin conceived, designed and supervised the study. Peng Chen, Lin Mei, Yunjie Chen and Xueqiang Guan researched the data. Lin Mei, Yunjie Chen, Shengqu He and Zhicheng Hu contributed to the discussion and design of the project. Yunjie Chen, Lin Mei, Cheng Jin, Huinan Chen, Zhicheng Hu, Yang Wang and Wanqian Li wrote the paper. Lin Mei and Yunjie Chen are the guarantor of this work and, as such, had full access to all the data in the study and takes responsibility for the integrity of the data and the accuracy of the data analysis. All authors read and approved the final manuscript.

Declaration of competing interest

The authors declare no competing interests.

Data availability

Data will be made available on request.

Acknowledgements

We acknowledge and appreciate our colleagues for their valuable suggestions and technical assistance for this study.

Appendix A. Supplementary data

Supplementary data to this article can be found online at <https://doi.org/10.1016/j.redox.2022.102468>.

References

- [1] S. Virani, A. Alonso, E. Benjamin, M. et al., Heart disease and stroke statistics-2020 update: a report from the American heart association, *Circulation* 141 (9) (2020) e139–e596, <https://doi.org/10.1161/CIR.0000000000000757>.
- [2] C.W. Tsao, A.W. Aday, Z.I. Almarzoq, et al., Heart disease and stroke statistics-2022 update: a report from the American heart association, *Circulation* 145 (8) (2022) e153–e639, <https://doi.org/10.1161/CIR.0000000000001052>.
- [3] D. McManus, J. Gore, J. Yarzebski, et al., Recent trends in the incidence, treatment, and outcomes of patients with STEMI and NSTEMI, *Am. J. Med.* 124 (1) (2011) 40–47, <https://doi.org/10.1016/j.amjmed.2010.07.023>.
- [4] J. Zweier, M. Talukder, The role of oxidants and free radicals in reperfusion injury, *Cardiovasc. Res.* 70 (2) (2006) 181–190, <https://doi.org/10.1016/j.cardiores.2006.02.025>.
- [5] H. Bugger, K. Pfeil, Mitochondrial ROS in myocardial ischemia reperfusion and remodeling, *Biochim. Biophys. Acta, Mol. Basis Dis.* 1866 (7) (2020), 165768, <https://doi.org/10.1016/j.bbadis.2020.165768>.
- [6] V. Sosa, T. Moliné, R. Somoza, et al., Oxidative stress and cancer: an overview, *Ageing Res. Rev.* 12 (1) (2013) 376–390, <https://doi.org/10.1016/j.arr.2012.10.004>.
- [7] M. Tomandlova, J. Parenica, P. Lokaj, et al., Prognostic value of oxidative stress in patients with acute myocardial infarction complicated by cardiogenic shock: a prospective cohort study, *Free Radic. Biol. Med.* (2021), <https://doi.org/10.1016/j.freeradbiomed.2021.07.040>.
- [8] N. Itoh, D. Ornitz, Fibroblast growth factors: from molecular evolution to roles in development, metabolism and disease, *J. Biochem.* 149 (2) (2011) 121–130, <https://doi.org/10.1093/jb/mvq121>.
- [9] S. Galiacy, E. Planus, H. Lepetit, et al., Keratinocyte growth factor promotes cell motility during alveolar epithelial repair *in vitro*, *Exp. Cell Res.* 283 (2) (2003) 215–229, [https://doi.org/10.1016/s0014-4827\(02\)00049-6](https://doi.org/10.1016/s0014-4827(02)00049-6).
- [10] Y. Xu, Y. Hong, M. Xu, et al., Role of keratinocyte growth factor in the differentiation of sweat gland-like cells from human umbilical cord-derived mesenchymal stem cells, stem cells transl. Med. *Times* 5 (1) (2016) 106–116, <https://doi.org/10.5966/sctm.2015-0081>.

- [11] S. Braun, C. Hanselmann, M. Gassmann, et al., Nrf2 transcription factor, a novel target of keratinocyte growth factor action which regulates gene expression and inflammation in the healing skin wound, *Mol. Cell Biol.* 22 (15) (2002) 5492–5505, <https://doi.org/10.1128/MCB.22.15.5492-5505.2002>.
- [12] I. Mason, F. Fuller-Pace, R. Smith, et al., FGF-7 (keratinocyte growth factor) expression during mouse development suggests roles in myogenesis, forebrain regionalisation and epithelial-mesenchymal interactions, *Mech. Dev.* 45 (1) (1994) 15–30, [https://doi.org/10.1016/0925-4773\(94\)90050-7](https://doi.org/10.1016/0925-4773(94)90050-7).
- [13] T. Huang, L. Wang, D. Liu, et al., FGF7/FGFR2 signal promotes invasion and migration in human gastric cancer through upregulation of thrombospondin-1, *Int. J. Oncol.* 50 (5) (2017) 1501–1512, <https://doi.org/10.3892/ijo.2017.3927>.
- [14] F. Pagano, F. Angelini, C. Castaldo, et al., Normal versus pathological cardiac fibroblast-derived extracellular matrix differentially modulates cardioprotection-derived cell paracrine properties and commitment, *Stem Cell. Int.* (2017), 7396462, <https://doi.org/10.1155/2017/7396462>.
- [15] J. Lopes, L. Dallan, S. Campana-Filho, et al., Keratinocyte growth factor: a new mesothelial targeted therapy to reduce postoperative pericardial adhesions, *Eur. J. Cardio. Thorac. Surg.* 35 (2) (2009) 313–318, <https://doi.org/10.1016/j.ejcts.2008.09.046>.
- [16] A. McDonnell, K. Lenz, Palifermin: role in the prevention of chemotherapy- and radiation-induced mucositis, *Ann. Pharmacother.* 41 (1) (2007) 86–94, <https://doi.org/10.1345/aph.1G473>.
- [17] D. Calcagno, R. Ng, A. Toomu, et al., The myeloid type I interferon response to myocardial infarction begins in bone marrow and is regulated by Nrf2-activated macrophages, *Sci. Immunol.* 5 (51) (2020), <https://doi.org/10.1126/sciimmunol.aaz1974>.
- [18] H. Ashrafian, G. Czibik, M. Bellahcene, et al., Fumarate is cardioprotective via activation of the Nrf2 antioxidant pathway, *Cell Metabol.* 15 (3) (2012) 361–371, <https://doi.org/10.1016/j.cmet.2012.01.017>.
- [19] Q. Chen, Nrf2 for cardiac protection: pharmacological options against oxidative stress, *Trends Pharmacol. Sci.* (2021), <https://doi.org/10.1016/j.tips.2021.06.005>.
- [20] S. Cadenas, Mitochondrial uncoupling, ROS generation and cardioprotection, *Biochim. Biophys. Acta Bioenerg.* 1859 (9) (2018) 940–950, <https://doi.org/10.1016/j.bbabi.2018.05.019>.
- [21] M.A. Al-Zeer, A. Xavier, M. Abu Lubad, et al., Chlamydia trachomatis prevents apoptosis via activation of PDPK1-MYC and enhanced mitochondrial binding of hexokinase II, *EBioMedicine* 23 (2017) 100–110, <https://doi.org/10.1016/j.ebiom.2017.08.005>.
- [22] G.S. Krasnov, A.A. Dmitriev, V.A. Lakunina, et al., Targeting VDAC-bound hexokinase II: a promising approach for concomitant anti-cancer therapy, *Expert Opin. Ther. Targets* 17 (10) (2013) 1221–1233, <https://doi.org/10.1517/14728222.2013.833607>.
- [23] D. Roberts, V. Tan-Sah, J. Smith, et al., Akt phosphorylates HK-II at Thr-473 and increases mitochondrial HK-II association to protect cardiomyocytes, *J. Biol. Chem.* 288 (33) (2013) 23798–23806, <https://doi.org/10.1074/jbc.M113.482026>.
- [24] E. Cheung, R. Ludwig, K. Vousden, Mitochondrial localization of TIGAR under hypoxia stimulates HK2 and lowers ROS and cell death, *Proc. Natl. Acad. Sci. U. S. A.* 109 (50) (2012) 20491–20496, <https://doi.org/10.1073/pnas.1206530109>.
- [25] Y. Zhu, L. Yang, Q.Y. Chong, et al., Long noncoding RNA Linc00460 promotes breast cancer progression by regulating the miR-489-5p/FGF7/AKT axis, *Cancer Manag. Res.* 11 (2019) 5983–6001, <https://doi.org/10.2147/CMAR.S207084>.
- [26] W. Chen, L. Wu, Y. Hu, et al., MicroRNA-107 ameliorates damage in a cell model of Alzheimer's disease by mediating the FGF7/FGFR2/PI3K/akt pathway, *J. Mol. Neurosci.* 70 (10) (2020) 1589–1597, <https://doi.org/10.1007/s12031-020-01600-0>.
- [27] S. Li, Z. Zhu, M. Xue, et al., The protective effects of fibroblast growth factor 10 against hepatic ischemia-reperfusion injury in mice, *Redox Biol.* 40 (2021), 101859, <https://doi.org/10.1016/j.redox.2021.101859>.
- [28] G. Lu, H.K. Haider, S. Jiang, et al., Sca-1+ stem cell survival and engraftment in the infarcted heart: dual role for preconditioning-induced connexin-43, *Circulation* 119 (19) (2009) 2587–2596, <https://doi.org/10.1161/CIRCULATIONAHA.108.827691>.
- [29] S. Liu, Y. He, J. Shi, et al., STAT1-activated LINC00961 regulates myocardial infarction by the PI3K/AKT/GSK3 β signaling pathway, *J. Cell. Biochem.* 120 (8) (2019) 13226–13236, <https://doi.org/10.1002/jcb.28596>.
- [30] S. Cheng, X. Zhang, Q. Feng, et al., Astragaloside IV exerts angiogenesis and cardioprotection after myocardial infarction via regulating PTEN/PI3K/Akt signaling pathway, *Life Sci.* 227 (2019) 82–93, <https://doi.org/10.1016/j.lfs.2019.04.040>.
- [31] H.K. Bryan, A. Olayanju, C.E. Goldring, et al., The Nrf2 cell defence pathway: keep1-dependent and -independent mechanisms of regulation, *Biochem. Pharmacol.* 85 (6) (2013) 705–717, <https://doi.org/10.1016/j.bcp.2012.11.016>.
- [32] Y. Liu, T. Lu, C. Zhang, et al., Activation of YAP attenuates hepatic damage and fibrosis in liver ischemia-reperfusion injury, *J. Hepatol.* 71 (4) (2019) 719–730, <https://doi.org/10.1016/j.jhep.2019.05.029>.
- [33] M. Ackers-Johnson, P.Y. Li, A.P. Holmes, et al., Langendorff-free method for concomitant isolation of viable cardiac myocytes and nonmyocytes from the adult mouse heart, *Circ. Res.* 119 (8) (2016) 909–920, <https://doi.org/10.1161/CIRCRESAHA.116.309202>.
- [34] Y. Kuwabara, T. Horie, O. Baba, et al., MicroRNA-451 exacerbates lipotoxicity in cardiac myocytes and high-fat diet-induced cardiac hypertrophy in mice through suppression of the LKB1/AMPK pathway, *Circ. Res.* 116 (2) (2015) 279–288, <https://doi.org/10.1161/CIRCRESAHA.116.304707>.
- [35] Y. Feng, W. Huang, W. Meng, et al., Heat shock improves Sca-1+ stem cell survival and directs ischemic cardiomyocytes toward a prosurvival phenotype via exosomal transfer: a critical role for HSF1/miR-34a/HSP70 pathway, *Stem Cell.* 32 (2) (2014) 462–472, <https://doi.org/10.1002/stem.1571>.
- [36] D. Kovacs, S. Raffa, E. Flori, et al., Keratinocyte growth factor down-regulates intracellular ROS production induced by UVB, *J. Dermatol. Sci.* 54 (2) (2009) 106–113, <https://doi.org/10.1016/j.jdermsci.2009.01.005>.
- [37] X. Luo, J. Zhou, Z. Wang, et al., An inhibitor role of Nrf2 in the regulation of myocardial senescence and dysfunction after myocardial infarction, *Life Sci.* 259 (2020), 118199, <https://doi.org/10.1016/j.lfs.2020.118199>.
- [38] S. Zhou, J. Wang, X. Yin, Y. et al., Nrf2 expression and function, but not MT expression, is indispensable for sulforaphane-mediated protection against intermittent hypoxia-induced cardiomyopathy in mice, *Redox Biol.* 19 (2018) 11–21, <https://doi.org/10.1016/j.redox.2018.07.014>.
- [39] S. Deng, K. Essandoh, X. Wang, et al., Tsg101 positively regulates P62-Keap1-Nrf2 pathway to protect hearts against oxidative damage, *Redox Biol.* 32 (2020), 101453, <https://doi.org/10.1016/j.redox.2020.101453>.
- [40] X. Li, D. Han, Z. Tian, et al., Activation of cannabinoid receptor type II by AM1241 ameliorates myocardial fibrosis via nrf2-mediated inhibition of TGF- β 1/smads3 pathway in myocardial infarction mice, *Cell. Physiol. Biochem.* 39 (4) (2016) 1521–1536, <https://doi.org/10.1159/000447855>.
- [41] S. Miyamoto, A.N. Murphy, J.H. Brown, Akt mediates mitochondrial protection in cardiomyocytes through phosphorylation of mitochondrial hexokinase-II, *Cell Death Differ.* 15 (3) (2008) 521–529, <https://doi.org/10.1038/sj.cdd.4402285>.
- [42] L. Amigoni, E. Martegani, S. Colombo, Lack of HXK2 induces localization of active Ras in mitochondria and triggers apoptosis in the yeast *Saccharomyces cerevisiae*, *Oxid. Med. Cell. Longev.* (2013), 678473, <https://doi.org/10.1155/2013/678473>.
- [43] A. Saraste, K. Pulkki, M. Kallajoki, et al., Apoptosis in human acute myocardial infarction, *Circulation* 95 (2) (1997) 320–323, <https://doi.org/10.1161/01.cir.95.2.320>.
- [44] H. Yaoita, K. Ogawa, K. Maehara, et al., Apoptosis in relevant clinical situations: contribution of apoptosis in myocardial infarction, *Cardiovasc. Res.* 45 (3) (2000) 630–641, [https://doi.org/10.1016/s0008-6363\(99\)00349-1](https://doi.org/10.1016/s0008-6363(99)00349-1).
- [45] W. Dröge, Free radicals in the physiological control of cell function, *Physiol. Rev.* 82 (1) (2002) 47–95, <https://doi.org/10.1152/physrev.00018.2001>.
- [46] M. Valko, D. Leibfritz, J. Moncol, et al., Free radicals and antioxidants in normal physiological functions and human disease, *Int. J. Biochem. Cell Biol.* 39 (1) (2007) 44–84, <https://doi.org/10.1016/j.biocel.2006.07.001>.
- [47] S.J. Dixon, B.R. Stockwell, The role of iron and reactive oxygen species in cell death, *Nat. Chem. Biol.* 10 (1) (2014) 9–17, <https://doi.org/10.1038/nchembio.1416>.
- [48] S. Ye, T. Zhao, W. Zhang, et al., p53 isoform Δ 113p53 promotes zebrafish heart regeneration by maintaining redox homeostasis, *Cell Death Dis.* 11 (7) (2020) 1–13, <https://doi.org/10.1038/s41419-020-02781-7>.
- [49] D.B. Lombard, K.F. Chua, R. Mostoslavsky, et al., DNA repair, genome stability, and aging, *Cell* 120 (4) (2005) 497–512, <https://doi.org/10.1016/j.cell.2005.01.028>.
- [50] H. Lv, Q. Liu, Z. Wen, et al., Xanthohumol ameliorates lipopolysaccharide (LPS)-induced acute lung injury via induction of AMPK/GSK3 β -Nrf2 signal axis, *Redox Biol.* 12 (2017) 311–324, <https://doi.org/10.1016/j.redox.2017.03.001>.
- [51] J.G. Pastorino, J.B. Hoek, Hexokinase II: the integration of energy metabolism and control of apoptosis, *Curr. Med. Chem.* 10 (16) (2003) 1535–1551, <https://doi.org/10.2174/0929867033457269>.
- [52] W.S. da-Silva, A. Gómez-Puyou, M.T. de Gómez-Puyou, et al., Mitochondrial bound hexokinase activity as a preventive antioxidant defense: steady-state ADP formation as a regulatory mechanism of membrane potential and reactive oxygen species generation in mitochondria, *J. Biol. Chem.* 279 (38) (2004) 39846–39855, <https://doi.org/10.1074/jbc.M403835200>.
- [53] L. Sun, S. Shukair, T.J. Naik, et al., Glucose phosphorylation and mitochondrial binding are required for the protective effects of hexokinases I and II, *Mol. Cell Biol.* 28 (3) (2008) 1007–1017, <https://doi.org/10.1128/MCB.00224-07>.
- [54] B. Munz, S. Frank, G. Hübner, et al., A novel type of glutathione peroxidase: expression and regulation during wound repair, *Biochem. J.* 326 (Pt 2) (1997) 579–585, <https://doi.org/10.1042/bj3260579>.
- [55] J. Sun, X. Huang, C. Niu, et al., aFGF alleviates diabetic endothelial dysfunction by decreasing oxidative stress via Wnt/ β -catenin-mediated upregulation of HXK2, *Redox Biol.* 39 (2021), 101811, <https://doi.org/10.1016/j.redox.2020.101811>.
- [56] W. Zhaohui, N. Yingli, L. Hongli, et al., Amentoflavone induces apoptosis and suppresses glycolysis in glioma cells by targeting miR-124-3p, *Neurosci. Lett.* 686 (2018) 1–9, <https://doi.org/10.1016/j.neulet.2018.08.032>.
- [57] L. Jiang, X. Yin, Y.H. Chen, et al., Proteomic analysis reveals ginsenoside Rb1 attenuates myocardial ischemia/reperfusion injury through inhibiting ROS production from mitochondrial complex I, *Theranostics* 11 (4) (2021) 1703–1720, <https://doi.org/10.7150/thno.43895>.
- [58] P.W. Finch, J.S. Rubin, T. Miki, et al., Human KGF is FGF-related with properties of a paracrine effector of epithelial cell growth, *Science* 245 (4919) (1989), <https://doi.org/10.1126/science.2475908>, 752–725.
- [59] L.C. Deng, T. Alinejad, S. Bellucci, et al., Fibroblast growth factors in the management of acute kidney injury following ischemia-reperfusion, *Front. Pharmacol.* 11 (2020) 426, <https://doi.org/10.3389/fphar.2020.00426>.
- [60] X. Shi, H.Y. Liu, S.P. Li, et al., Keratinocyte growth factor protects endometrial cells from oxygen glucose deprivation/re-oxygenation via activating Nrf2 signaling, *Biochem. Biophys. Res. Commun.* 501 (1) (2018) 178–185, <https://doi.org/10.1016/j.bbrc.2018.04.208>.
- [61] T. Sadohara, K. Sugahara, Y. Urashima, et al., Keratinocyte growth factor prevents ischemia-induced neuronal death in the hippocampal CA1 field of the gerbil brain, *Neuroreport* 12 (1) (2001) 71–76, <https://doi.org/10.1097/00001756-200101220-00022>.

- [62] C. Vinsonneau, A. Girshovich, B. M'Rad M, et al., Intrarenal urothelium proliferation: an unexpected early event following ischemic injury, *Am. J. Physiol. Ren. Physiol.* 299 (3) (2010) F479–F486, <https://doi.org/10.1152/ajprenal.00585.2009>.
- [63] T. Ichimura, P.W. Finch, G. Zhang, et al., Induction of FGF-7 after kidney damage: a possible paracrine mechanism for tubule repair, *Am. J. Physiol.* 271 (5 Pt 2) (1996) F967–F976, <https://doi.org/10.1152/ajprenal.1996.271.5.F967>.
- [64] A. Beenken, M. Mohammadi, The FGF family: biology, pathophysiology and therapy, *Nat. Rev. Drug Discov.* 8 (3) (2009) 235–253, <https://doi.org/10.1038/nrd2792>.
- [65] S. Frank, B. Munz, S. Werner, The human homologue of a bovine non-selenium glutathione peroxidase is a novel keratinocyte growth factor-regulated gene, *Oncogene* 14 (8) (1997) 915–921, <https://doi.org/10.1038/sj.onc.1200905>.
- [66] D.J. Pennisi, T. Mikawa, Normal patterning of the coronary capillary plexus is dependent on the correct transmural gradient of FGF expression in the myocardium, *Dev. Biol.* 279 (2) (2005) 378–390, <https://doi.org/10.1016/j.ydbio.2004.12.028>.
- [67] C.J. Morabito, R.W. Dettman, J. Kattan, et al., Positive and negative regulation of epicardial-mesenchymal transformation during avian heart development, *Dev. Biol.* 234 (1) (2001) 204–215, <https://doi.org/10.1006/dbio.2001.0254>.
- [68] P. Yu, K. Wilhelm, A. Dubrac, et al., FGF-dependent metabolic control of vascular development, *Nature* 545 (7653) (2017) 224–228, <https://doi.org/10.1038/nature22322>.
- [69] Y. Mao, X. Chen, Y. Xia, et al., Repair effects of KGF on ischemia-reperfusion-induced flap injury via activating Nrf2 signaling, *J. Surg. Res.* 244 (2019) 547–557, <https://doi.org/10.1016/j.jss.2019.06.078>.
- [70] A. Giacomini, S. Taranto, S. Rezzola, et al., Inhibition of the FGF/FGFR system induces apoptosis in lung cancer cells via c-Myc downregulation and oxidative stress, *Int. J. Mol. Sci.* 21 (24) (2020) 9376, <https://doi.org/10.3390/ijms21249376>.
- [71] X. Chen, P. Zhabayev, A.K. Azad, et al., Pharmacological and cell-specific genetic PI3K α inhibition worsens cardiac remodeling after myocardial infarction, *J. Mol. Cell. Cardiol.* 157 (2021) 17–30, <https://doi.org/10.1016/j.yjmcc.2021.04.004>.
- [72] A. Tsang, D.J. Hausenloy, M.M. Mocanu, et al., Postconditioning: a form of "modified reperfusion" protects the myocardium by activating the phosphatidylinositol 3-kinase-Akt pathway, *Circ. Res.* 95 (3) (2004) 230–232, <https://doi.org/10.1161/01.RES.0000138303.76488.fe>.
- [73] Y. Xin, Y. Bai, X. Jiang, et al., Sulforaphane prevents angiotensin II-induced cardiomyopathy by activation of Nrf2 via stimulating the Akt/GSK-3 β /Fyn pathway, *Redox Biol.* 15 (2018) 405–417, <https://doi.org/10.1016/j.redox.2017.12.016>.
- [74] S. Chowdhry, Y. Zhang, M. McMahon, et al., Nrf2 is controlled by two distinct β -TrCP recognition motifs in its Neh6 domain, one of which can be modulated by GSK-3 activity, *Oncogene* 32 (32) (2013) 3765–3781, <https://doi.org/10.1038/onc.2012.388>.